The nearshore cradle of early vertebrate diversification

DOI:
10.1126/science.aar3689

Document Version
Accepted author manuscript

Title: The nearshore cradle of early vertebrate diversification.

Authors: Lauren Sallan[1a*], Matt Friedman[2], Robert S. Sansom[3], Charlotte M. Bird[4], Ivan J. Sansom[4a*]

Affiliations:

[1]Department of Earth and Environmental Science, University of Pennsylvania, Philadelphia, Pennsylvania 19104.

[2]Museum of Paleontology, University of Michigan, Ann Arbor, MI 48109.

[3]School of Earth and Environmental Sciences, University of Manchester, Manchester, M13 9PT UK.

[4]School of Geography, Earth and Environmental Sciences, University of Birmingham, Birmingham, B15 2TT UK.

[a] These authors contributed equally.

[*]Correspondence to: lsallan@upenn.edu, i.j.sansom@bham.ac.uk

Abstract: Ancestral vertebrate habitats are subject to controversy, and obscured by limited, often contradictory, paleontological data. We assembled fossil vertebrate occurrence and habitat datasets spanning the mid-Paleozoic (480-360 Mya) and found that early vertebrate clades, both jawed and jawless, originated in restricted, shallow intertidal-subtidal environments. Nearshore divergences gave rise to body plans with different dispersal abilities: robust fishes shifted more shoreward while gracile groups moved seaward. Freshwaters were invaded repeatedly, but movement to deeper waters was contingent upon form, and short-lived until the later Devonian. Our results contrast with the onshore-offshore trends, reef-centered diversification, and mid-shelf clustering observed in benthic invertebrates. Nearshore origins for vertebrates may be linked to the demands of their mobility, and influenced the structure of their early fossil record and diversification.

One sentence summary: Early vertebrates diversified in restricted, shallow marine waters, with nearshore divergence in body form shaping their dispersal and fossil record.

The ancestral habitat of vertebrates has long been debated, with opinions ranging from freshwater to open ocean (*1-3*). Inferences have been derived from either the evolutionarily-distant modern fauna or qualitative narratives based on select fossils. Early records of vertebrate divisions, such as jawed fishes and their relatives (total-group gnathostomes), consist of long gaps between inferred origination and definitive appearances (ghost lineages), punctuated by suggestive microfossils (*4-7*). Vertebrates, apart from tooth-like conodont elements, were restricted in Ordovician ecosystems as trivial components of the Great Ordovician Biodiversification Event (*4, 5, 7*). Ancestral habitat is a critical factor in determining both pattern and mode of diversification, potential mismatches between biodiversity and available habitat area, and the source of apparent relationships with changing sea level (*6*). A lack of early vertebrate fossil data and habitat information in compendia has limited quantitative approaches (*4*), preventing resolution of this outstanding issue in vertebrate evolution.

We developed a database of total-group gnathostome occurrences (~480-360 My; *4, 5, 8*) during their mid-Paleozoic diversification (n=1421; *9*; Fig. S1). Data collection focused on all occurrences from the interval encompassing the five oldest localities for each major clade (n=188, Fig. 1, Figs. S1, S2) and phylogenetically-constrained genera within jawless groups (n=785; Figs 2, 3; Figs. S1, S3, S4) for use with Bayesian ancestral state reconstruction. We used environmental, lithological, and invertebrate community information from the literature and available databases to assign occurrences to Benthic Assemblage zones (*10;* Fig. 1). Benthic Assemblage zones are categorized and ordered as freshwater (BA0), intertidal above typical wave base (BA1), shallow subtidal/lagoon (BA2), deeper subtidal, including the start of tabulate coral-stromatoporoid reef systems

68 (BA3), mid- to outer-shelf zone (BA4 and BA5) and shelf margin towards the bathyal
69 region (BA6) and have been widely used in studies of mid-Paleozoic paleocommunities
70 (*1, 10-12*) (Fig. 1).

71 We applied Bayesian threshold models to phylogenies of occurrences using prior
72 probabilities of residence in each Benthic Assemblage zone. This allowed positive
73 inference of both ancestral habitats and amount of evolutionary change required to move
74 between zones ("liability" values; *13*). All major clades, from the first skeletonizing
75 jawless fishes (astraspids, arandaspids) to jawed bony fishes (osteichthyans), originated
76 within nearshore intertidal and subtidal zones (~BA1-3), centered on BA2, over a period
77 of more than 100 million years (Fig. 1A, fig. S3). This area is relatively shallow, includes
78 lagoons in reefal systems, and is located entirely above storm wave base in the mid-
79 Paleozoic (*11)*(Fig. 1).

80 We appraised whether nearshore origination in gnathostomes resulted from
81 environmental bias in the record through comparison with habitat distributions for other
82 facets of the mid-Paleozoic captured in independent datasets, including fossiliferous
83 strata, regional paleocommunities, and global occurrences and richness (number of
84 genera) (Fig. 1B; figs. S11-S16) (*10, 14*). Analysis of mid-Paleozoic strata in the
85 Paleobiology Database (PBDB; *14*), binned by distinct habitat categories (n=4437),
86 produced a distribution clustered on deep subtidal/reef environments (equivalent to
87 BA3/4 (*10*)) with many fewer records in freshwater-marginal marine (BA0-1) and the
88 basin/slope (~BA5/6) (Fig. 1B, figs. S11, S12). PBDB records of occurrences (n=111364)
89 or genera (n=24211) provide distributions that show even greater clustering on the mid-
90 shelf, but are highly correlated with sampled strata (linear regression: r^2=0.96, p=0.0004

and r^2=0.94; p=0.0008 respectively, fig. S12). Silurian and Lochkovian regional paleocommunities (*10*) are also centered on BA3-4 (Fig. 1B, fig. S13). These records suggest a global, mid-shelf center for sampling and diversity, and a null expectation of originations in deep subtidal and reef environments (more so than expected from previous studies focused on reef-bearing facies (*15*)). This is in stark contrast with shallower gnathostome ancestral habitats (Fig. 1), which is thus unlikely to result from global sampling bias.

Testing whether apparent nearshore origination resulted from preservational biases in different habitats, we compared gnathostome distributions to Paleobiology Database records for conodonts. Conodonts are the sister group of extant jawless cyclostomes or the vertebrate total-group, largely known from phosphatic oral elements (*4*) which serve as an independent preservational proxy. Conodonts are stratigraphic index fossils and common along the marine depth gradient during the mid-Paleozoic (Fig. 1B, fig. S14). Conodont occurrences (n=11915) show a different distribution from other Paleobiology Database records (Chi-squared p<0.0001), exhibiting a peak in BA2 and more occurrences in BA5/6 (Figs. S14, S15). Conodont richness (n=1308) is more clustered around BA3/4, particularly in the Silurian-Lochkovian (n=505)(Fig. 1B, figs. S14, S15). This pattern argues against early gnathostome restriction resulting from preservational bias, as does the plurality of vertebrate occurrences in deeper waters from the early Silurian (Fig. 1C, fig. S1).

Jawed and jawless fish distributions are highly clustered in BA0-2 early in clade history (n=478), in the Silurian and Lochkovian (n=1035), and over the mid-Paleozoic (n=2147) (Fig. 1, figs. S1, S16-S18). We recover no significant or strong, positive

114 correlations between this gnathostome pattern and other fossil records (linear regression
115 r^2 range: -0.90-0.27, p-range: 0.41-0.9) (Fig. 1B, fig. S16).
116 Ancestral states show that gnathostomes originated preferentially nearshore, even
117 as diversity of species and body forms increased (Fig. 1A, fig. S2). Early occurrences are
118 significantly different from later records within groups (Chi-squared p=<0.00001)(Fig.
119 1C, fig. S18); gnathostomes as a whole, as well as jawed and jawless fishes specifically,
120 exhibit greater clustering in shallow marine settings (BA1-2) independent of exact time
121 of first appearance in the mid-Paleozoic (Fig. 1C, fig. S18). Shallow ancestral habitats are
122 always supported by our analyses despite variation in first appearances of jawed fishes
123 (e.g. inclusion of potential Ordovician "chondrichthyan" material; *15*), placoderm
124 monophyly or paraphyly (*8),* and even increasing the minimum prior probability of
125 occurrences in all zones to a minimum of 5% or 10% to account for potential of false
126 absence, missing records or other sampling issues (Fig. 1A, figs. S2-S5; Table S1).
127 Gnathostomes continued to show a strong tendency to diverge in shallow marine waters
128 long after the invasion of deeper and freshwaters by older lineages, including after the
129 origin of jaws.
130 Threshold liability values suggest that shifts within the nearshore waters required
131 little evolutionary change and were common, as was invasion of freshwater (Table 1; Fig.
132 1C). Dispersal into deeper waters, including the forereef, shelf and open ocean (BA4-6),
133 was more restricted (Table 1), complicated by a short term tendency to return to the
134 ancestral shallows (Ornstein-Uhlenbeck, DIC weight=1; phylogenetic half-life in Table
135 1)(*16*). Yet, threshold values also suggest rapid dispersal across the offshore shelf (BA4-5)
136 once lineages managed to depart BA3, even though shifts into open waters (BA6) had

much higher requirements (Table 1). However, if sampling probabilities in all bins is increased *a priori*, shallow-water restriction of early gnathostomes is explained by ever-higher thresholds for continued movement offshore, starting at BA2 (Fig. 1A, figs. S2-S5; Table S1).

Next, determined the association between body form and dispersal ability within major groups. Clades were categorized into two body forms: 1) macromeric, which are mostly robust and armored with large bony plates (e.g. heterostracans, osteostracans, galeaspids)(*17*)(Fig. 2) or 2) micromeric, which are mostly gracile and either naked or covered in small scales (e.g. thelodonts and anaspids)(*17*)(Fig. 3). These robust or gracile forms can be approximated as having benthic or pelagic/nektonic lifestyles, respectively, given gross similarity to living fishes (*18, 19*).

Analysis of all gnathostome early occurrences shows that both micromeric and macromeric forms originated around shallow water BA2 (Fig. 1A, S2). However, group-level analyses suggest that slight shifts shoreward or seaward preceded the later diversification of these groups. Genus-level diversification of macromeric jawless lineages was centered in the shallows (BA1-2) and freshwater (BA0) throughout their multi-million-year existence (Fig. 2, figs. S6-S8, S19, S20). Later occurrences were significantly more clustered in shallow and freshwater settings than the earliest members of these clades (Chi-Squared $p<0.0001$) (Fig. 2C, figs. S19, S20). Threshold values indicate moving into deeper waters was more difficult for robust groups than gnathostomes as a whole (Tables 1, S1, S2), and these featured a strong tendency to return to the shallows (OU DIC weight range=0.99-1; phylogenetic half-life in Table 1).

159 The diversification of micromeric gnathostomes was centered in deeper subtidal
160 waters (BA3) following their origination in BA2 (Figs. 1A, 3, figs. S9, S10, S21, S22).
161 Early occurrences of these clades show a significantly greater concentration in BA1-2
162 than later forms (Chi-squared $p<0.0001$)(Fig. S21, S22). A handful of early Silurian
163 thelodont taxa were already resident in deeper waters (BA3-5), following their Late
164 Ordovician appearances in BA1-2 (Fig. S21A). Early dispersal into deeper waters reflects
165 low threshold parameters (Table 1), and may be a general pattern for gracile clades.
166 Jawed fishes show a significant shift onto reefs and deeper settings in the later Devonian
167 (Chi-squared $p<0.0001$)(Fig. 1C, figs. S1, S18), after the appearance of most subclades.
168 Robust jawless groups contain exceptions that may prove this rule; a few subclades with
169 fusiform bodies originated in BA3 and register deeper water occurrences than their
170 relatives by the mid-Silurian (e.g. trematapsid osteostracans)(Fig. 2, figs. S6-S8).
171 Dispersal in multiple directions appears to have been enabled by body form
172 evolution, rather than preceding the origin of new phenotypes in new habitats. These
173 shifts affected subsequent survival. Freshwater habitats were marked by the persistence
174 of robust clades like osteostracans and gracile forms like anaspids, without further
175 changes to gross body plan (Figs 2, 3). Sometimes identical deep-water lineages appear
176 short-lived and did not exhibit apparent further diversification, even on reefs (Fig. 1; *20*).
177 Jawless gnathostomes show a significant shift in distribution (Chi-Squared $p<0.00001$)
178 back into the ancestral nearshore habitats and adjacent estuarine areas following a peak in
179 distribution across the depth gradient in the Silurian to Early Devonian (Fig. 1C, figs. S1,
180 S18). This occurred just as jawed fishes moved out of nearshore habitats in the Devonian

(Fig. 1A, fig. S18)(*4,21*). This pattern is reflected in the greater representation of benthic forms in later marine jawless fishes vs "nektonic" forms in jawed vertebrates (*22*).

Overall, results show that the nearshore served as the cradle of early vertebrate taxonomic and gross morphological diversification (Figs 1-3). Specific body forms evolved in coastal waters subsequently favoring expansion into shallower (e.g. macromeric jawless fishes) or deeper areas (e.g. micromeric jawless fishes, jawed fishes). This mirrors observations within living fishes of repeated splits into benthic and pelagic/nektonic forms (*18, 23*), and the gross division of fish phenotype-environment associations (*19*).

A persistent diversification center within the shallows may explain features of the early vertebrate record (*7, 24*). Ordovician gnathostomes are primarily represented by microfossils restricted to a small subset of nearshore facies (Fig. S1) subject to wave action (*11*), despite worldwide distributions (*4, 7, 17, 24*). Ghost lineages for gnathostomes might be caused by environmental endemicity, low abundance, and/or a relative lack of marginal marine strata (Figs. S1, S11-S13). Alternatively, a relationship between Ordovician diversity and sea level (*6*) might have a common cause in changing shallow habitat area; reduction in such environments would have delayed apparent diversification and increased extinction risk (*6, 25, 26*).

Endemicity in coastal waters may have later promoted origination of new clades. Biogeographic patterns suggest that body-form divergence occurred in multiple shallow settings, increasing overall diversity. Micromeric forms occur alongside macromeric astraspids in the Ordovician of Laurentia, while robust galeaspids existed alongside gracile chondrichthyans in the early Silurian of Gondwana (*4-7,15, 17, 24, 27, 28*).

Nektonic body plans developed in these hotspots enabled dispersal across deep early Silurian oceans, away from local competition, leading to further diversification in nearshore settings elsewhere (*1, 15, 28*). In contrast, benthic groups showed structured geographic patterns (*27*), moving along coastlines and inshore, perhaps towards nutrient inputs essential to their likely bottom-feeding and filtering lifestyles and away from increased competition. Thus, continuous origination in shallow waters shaped the evolution of vertebrates during, at least, their first phase of diversification.

References and Notes

1. A. J, Boucot, C. Janis, The environment of the early Paleozoic vertebrates. *Paleogeogr. Paleoclimat. Palaeoecol.* **41**, 251-287 (1983).

2. T. C. Chamberlin, On the habitat of early vertebrates. *J. Geol.* **8**, 400- 412 (1900).

3. G. Carrete-Vega, J. J. Wiens, Why are there so few fish in the sea? *Proc. R. Soc. Lond. B* **279**, 2323-2329 (2012).

4. M. Friedman, L. C. Sallan, Five hundred million years of extinction and recovery: a Phanerozoic survey of large-scale diversity patterns in fishes. *Palaeontology* **55**,707-742 (2012).

5. I. J. Sansom, P. Andreev, The Ordovician enigma: fish, first appearances and phylogenetic controversies *In* Z. Johanson, M. Richter, C. Underwood, eds. Evolution and Development of Fishes (in press). (Cambridge Uni. Press)

6. R. S. Sansom, E. Randle, P. C. J. Donoghue, Discriminating signal from noise in the fossil record of early vertebrates reveals cryptic evolutionary history. *Proc. R. Soc. Lond. B* **282**, 20142245 (2015).

7. N. S. Davies, I. J. Sansom, Ordovician vertebrate habitats: a Gondwanan perspective. *Palaios* **24**, 717-722 (2009).

8. M. D. Brazeau, M. Friedman, The origin and early phylogenetic history of jawed vertebrates. *Nature* **520**, 490-497 (2015).

9. Materials and methods are available as supplementary materials on *Science* online.

10. A. Boucot, J. Lawson, eds, *Paleocommunities: A Case Study from the Silurian and Lower Devonian* Cambridge University: Cambridge (1999).

11. C. E. Brett, A. J. Boucot, B. Jones, Absolute depths of Silurian benthic assemblages. *Lethaia* **26**, 25-40 (1993).

12. H. Armstrong, D. A. T. Harper, An earth system approach to understanding the end-Ordovician (Hirnantian) mass extinction. *Geol. Soc. America Spec. Papers* **505,** 287-300 (2014)

13. L. K. Revell, Ancestral character estimation under the threshold model from quantitative genetics. *Evolution* **68**, 743-759 (2014).

14. Data downloaded from the Paleobiology Database (Paleobiodb.org) June 6-12, 2018.

15. P. S. Andreev, et al. *Elegestolepis* and its kin, the earliest monodontode chondrichthyans. *J. Vertebr. Paleontol.* **37**, e1245664 (2017).

16. T. F. Hansen, Stabilizing selection and the comparative analysis of adaptation. *Evolution* **51**, 1341-1351 (1997).

17. P. Janvier, *Early Vertebrates* Oxford University (1996).

18. D. Schluter, *The Ecology of Adaptive Radiation* Oxford University (2000).

19. T. Claverie, P. C. Wainwright, A morphospace for reef fishes: elongation is the dominant axis of body shape evolution. *PLoS ONE* **9**, e112732 (2014).

20. W. Kiessling, C. Simpson, M. Foote Reefs as cradles of evolution and sources of biodiversity in the Phanerozoic. *Science* **327**, 196-198 (2010).

21. P. S. L. Anderson, M. Friedman, M. D. Brazeau, E. Rayfield, Initial radiation of jaws demonstrated stability despite faunal and environmental change. *Nature* **476**, 206–209 (2011).

22. C. B. Klug, et al. The Devonian nekton revolution. *Lethaia* **43,** 465-477 (2010).

23. R. B. Langerhans, Predictability of phenotypic differentiation across flow regimes in fishes. *Integr Comp Biol* **48**, 750-768 (2008).

24. M. P. Smith, P. C. J. Donoghue, I. J. Sansom, The spatial and temporal diversification of Early Palaeozoic vertebrates. *Geol. Soc. London Spec. Publ.* **194**, 69-72 (2002).

25. B. Hannisdal, S. E. Peters, Phanerozoic Earth system evolution and marine biodiversity. *Science* **334**, 1121-1124 (2011).

26. C. Pimiento, et al., The Pliocene marine megafaunal extinction and its impact on functional diversity. *Nature Ecology and Evolution* **1,** 1100-1106 (2017).

27. R. S. Sansom, Endemicity and palaeobiogeography of the Osteostraci and Galeaspida: a test of scenarios of gnathostome evolution. *Palaeontology* **52**, 1257-1273 (2009).

28. T. Märss, S. Turner, V. Karatajute-Talimaa, "Agnatha" II: Thelodonti in H. P. Schultze Ed. *Handbook of Paleoichthyology* **Vol. 1B** Dr. Friedrich Pfeil: 1-143 (2007).

29. F. M. Gradstein, J. G. Ogg, M. Schmitz, G. Ogg, *The Geologic Time Scale 2012* (Elsevier, 2012).

30. A. J. Boucot, *Evolution and extinction rate controls* (Elsevier, 1975).

31. R. Plotnick, "Llandoverian-Lochkovian eurypterid communities," in *Paleocommunities: A Case Study from the Silurian and Lower Devonian*, A. Boucot, J. Lawson, Eds. (Cambridge Univ. Press, 1999), pp. 106-131.

32. W. P. Maddison, D. R. Maddison, Mesquite: a modular system for evolutionary analysis. Version 3, http://mesquiteproject.org (2017)

33. R. S. Sansom, K. Freedman, S. E. Gabbott, R. A. Aldridge, M. A. Purnell, Taphonomy and affinity of an enigmatic Silurian vertebrate *Jamoytius kerwoodi* White. *Palaeontology* **53**, 1393-1409 (2010).

34. M. Zhu, X. B. Yu, P. E. Ahlberg, B. Choo, J. Lu, T. Qiao, Q. M. Qu, W. J. Zhao, L. T. Jia, H. Blom, Y. A. Zhu, A Silurian placoderm with osteichthyan-like marginal jaw bones. *Nature* **502**, 188-193 (2013).

35. J. N. Keating, P. C. J. Donoghue, Histology and affinity of anaspids, and the early evolution of the vertebrate dermal skeleton. *Proc. R. Soc. Lond. B* **283**, 20152917 (2016).

36. J. Lu, S. Giles, M. Friedman, M. Zhu, A new stem-sarcopterygian illuminates patterns of character evolution in early bony fishes. *Nature Communications* **8,** 1932 (2017)

37. B. L. King, Bayesian morphological clock methods resurrect placoderm monophyly and reveal rapid early evolution in jawed vertebrates. *Syst. Biol.* **66**, 499–516 (2017).

38. R. S. Sansom, S. A. Rodygin, P. C. J. Donoghue, The anatomy, affinity and phylogenetic significance of *Ilemoraspis kirkinskayae* (Osteostraci) from the Devonian of Siberia. *J. Vert. Paleont.* **28**, 613-625 (2008).

39. R. S. Sansom, Phylogeny, classification and character polarity of the Osteostraci (Vertebrata). *J. Syst. Paleont.* **7**, 95-115 (2009).

40. M. V. H. Wilson, T. Märss, Thelodont phylogeny revisited, with inclusion of key scale-based taxa. *Eston. J. Earth Sci.* **58**, 297-310 (2009).

41. E. Randle, R. S. Sansom, Phylogenetic relationships of the 'higher heterostracans' (Heterostraci: Pteraspidiformes and Cyathaspididae), extinct jawless vertebrates. *Zool. J. Linn. Soc.* **zlx025** (2017).

42. M. Zhu, Z. Gai, Phylogenetic relationships of galeaspids (Agnatha). *Front. Biol. China* **2**, 1–19 (2007).

43. H. Blom, New birkeniid anaspid from the Lower Devonian of Scotland and its phylogenetic implications. *Palaeontology* **55**, 641-652 (2012).

44. P. C. J. Donoghue, M. A. Purnell, R. J. Aldridge, S. Zhang, The interrelationships of 'complex' conodonts (Vertebrata). *J. Syst. Palaeontol.* **6**, 119-153 (2008).

45. M. A. Bell, G. T. Lloyd, Strap: An R package for plotting phylogenies against stratigraphy and assessing their stratigraphic congruence, *Palaeontology* **58**, 379-389 (2015).

46. J. C. Uyeda, T. F. Hansen, S. J. Arnold, J. Pienaar, The million year wait for macroevolutionary bursts. *Proc. Natl. Acad. Sci. USA* **108,** 15908-15913 (2011).

47. L. J. Revell, phytools: an R package for phylogenetic comparative biology (and other things). *Methods Ecol. Evol.* **3**, 217-233 (2012).

48. G. E. Uhlenbeck, L. S. Ornstein, On the theory of Brownian Motion *Phys. Rev.* **36**, 823-841 (1930)

49. R. Lande, 1976. Natural selection and random drift in phenotypic evolution. *Evolution* **30,** 314-334 (1976).

50. M. Pagel, Inferring the historical patterns of biological evolution. *Nature* **401,** 877-884 (1999).

51. D. Spiegelhalter, N. G. Best, B. P. Carlin, A. van der Linde, Bayesian measures of model complexity and fit (with discussion). *J. Roy. Stat. Soc. B* **64,** 583-639 (2002).

52. K. P. Burnham, D. R. Anderson, *Model Selection and Multimodel Inference: A Practical Information-Theoretic Approach* (Springer, 2002).

53. D.-G. Shu, *et al*., Lower Cambrian vertebrates from south China. *Nature* **402**, 42–46 (1999)

54. I. J. Sansom, M. P. Smith, M. M. Smith, Scales of thelodont and shark-like fishes from the Ordovician. *Nature* **379**, 628-620 (1996).

55. I. J. Sansom, N. S. Davies, M. I. Coates, M. I., R. S. Nicoll, A. Ritchie, Chondrichthyan-like scales from the Middle Ordovician of Australia. *Palaeontology* **55**, 243–247 (2012)),

56. Z. Gai, P. C. J. Donoghue, M. Zhu, P. Janvier, M. Stampanoni, Fossil jawless fish from China foreshadows early jawed vertebrate anatomy. *Nature* **476**, 324-327 (2011).

57. I. J. Sansom, D. K. Elliott, A thelodont from the Ordovician of Canada. *J. Vert. Paleont.* **22**, 867-870 (2002).

58. R. J. Aldridge, S. E. Gabbott, J. N. Theron, "The Soom Shale," in: *Palaeobiology II* D. E. G. Briggs, P. R. Crowther, Eds (Blackwell, 2001), pp. 340-342.

59. D. J. E. Murdock, X.-P. Dong, J. E. Repetski, F. Marone, M. Stampanoni, P. C. J. Donoghue, The origin of conodonts and of vertebrate mineralized skeletons. *Nature* **502**, 546–549 (2013)).

60. J. R. Wheeley, P. E. Jardine, R. J. Raine, I. Boomer, M. P. Smith, Paleoecologic and paleoceanographic interpretation of δ18O variability in Lower Ordovician conodont species. *Geology* **46**, 467-470 (2018

Acknowledgements: We thank Z. Min, for assistance with galeaspid occurrences; L. Revell, G, Lloyd, J. Mitchell for advice on phylogenetic methods, S.Wang for assistance with statistical tests, N. Tamura for providing the reconstructions used in Figures 1-3, and D. Fraser and two anonymous reviewers for comments. **Funding:** University of Pennsylvania (L.S.), Palaeontological Association Undergraduate Research Bursary (C.M.B), University of Birmingham (I.J.S). **Author Contributions:** L.S. and I.J.S. designed the study, assembled the figures, interpreted results, and drafted the manuscript. L.S., R.S.S., C.M.B., and I.J.S. contributed data. L.S. performed analyses. L.S., M.F., R.S.S., C.M.B., and I.J.S. participated in designing analyses, discussion of results, and editing of the manuscript. **Competing Interests**: None Declared. **Data and Materials Availability:** All data are available in the supplementary materials and on Dryad at doi:10.5061/dryad.g08m87q.

Table 1. Best-Fit Model Parameters for Ancestral Habitats in Figures 1-3.

AncThresh (*13*) holds the threshold for exiting BA0 constant at 0 and BA6 as Infinity.

Values for parameters are means after excluding "burn-in." See Figs. S2-S10 and Database S1 for ancestral states.

Clade	Mean Threshold Liabilities (20 mil. gen., 20% burn-in)							Log Likelihood	*Alpha*	Half-life (My)
	BA0	BA1	BA2	BA3	BA4	BA5	BA6			
Gnathostomes	0	2.09	3.98	6.24	6.81	97.48	Inf	-657.77	0.13	5.33
Heterostracans	0	2.92	3.86	7.74	38.20	200.13	Inf	-979.86	0.12	5.78
Galeaspids	0	3.31	5.91	15.53	83.03	200.55	Inf	-446.63	0.01	138.63
Osteostracans	0	1.13	2.90	26.27	51.66	94.34	Inf	-433.09	0.08	8.66
Anaspids	0	0.19	0.34	1.35	1.40	103.24	Inf	-142.24	1.95	0.36
Thelodonts	0	0.61	0.93	2.05	2.15	110.77	Inf	-220.20	0.59	1.17

Figure Legends:

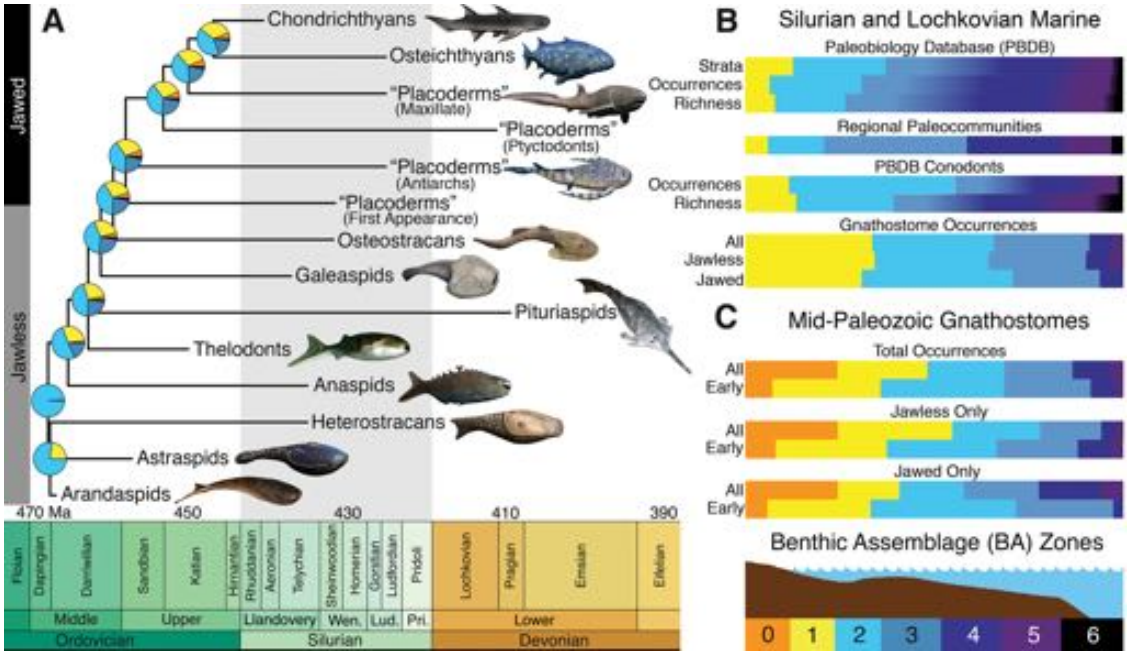

Figure 1. Mid-Paleozoic vertebrates preferentially originated in shallow marine habitats. A) Intertidal (BA1) to subtidal (BA2-3) ancestral habitats for total-group gnathostome clades (n=188) assuming placoderm paraphyly and Silurian first occurrence for chondrichthyans. Full results shown in Figs. S2-S5. B) Silurian and Lochkovian marine distributions for Paleobiology Database fossiliferous strata (n=858), richness (n=6980) and occurrences (n=30004), conodont richness (n=505) and occurrences (n=7447), paleocommunities, (n=2401) and gnathostome occurrences (n=1035) show mid-Paleozoic records peaking on the mid-shelf (BA3-4) with few records in marginal marine settings, in contrast to the shallow water preferences of early gnathostomes. C) Early and overall occurrences for total-group gnathostomes (n=2827), jawed fishes (n=1343) and jawless fishes (n=1484) show that early occurrences were significantly more concentrated in shallow marine settings than overall or later occurrences. See Additional Data File S2 and Figs. S1, S5-S9

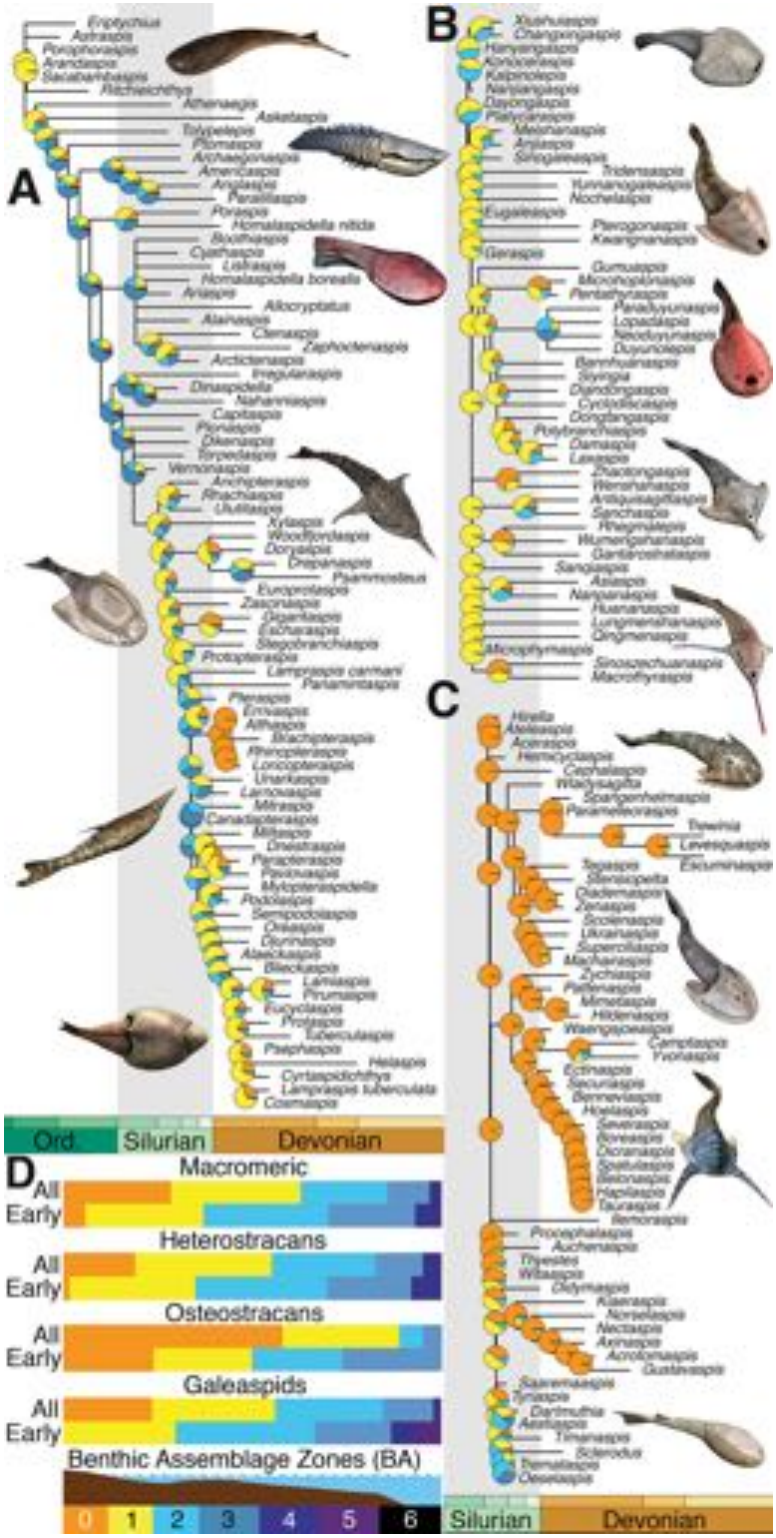
A
B
C
D
Ord
Silurian
Devonian
Macromeric
All
Early
Heterostracans
Osteostracans
Galeaspids
Benthic Assemblage Zones (BA)
0
1
2
3
4
5
6
Silurian
Devonian

Figure 2. Macromeric, robust jawless fishes exhibit shallower-water diversification and greater habitat restriction. Ancestral states for A) heterostracans and Ordovician stem-gnathostomes (n=316), B) galeaspids (n=112), and C) osteostracans (n=158) show that macromeric genera preferentially originated in very shallow waters (BA0-2) with the exception of more streamlined forms. Full results shown in Figs S6-S8. D) Early and later habitat distributions for macromeric clades (n=1123) showing significant shifts towards shallower water subsequent to their origination. Full distributions shown in Figs. S19 and S20 and Additional Data File S1.

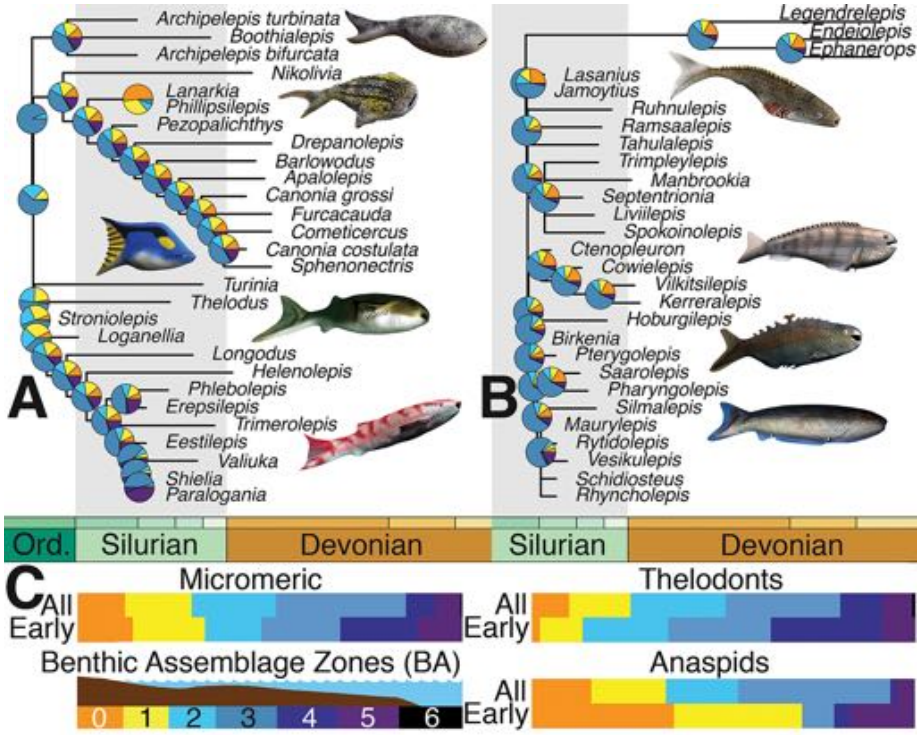

Figure 3. Micromeric, gracile jawless fishes exhibit deeper-subtidal later diversification and easier dispersal. Ancestral states for A) thelodonts (n=99), B) anaspids (n=100) showing diversification of genera in deeper subtidal waters during their evolutionary history. Full results shown in Figs. S9 and S10. C) Early and later occurrences for micromeric jawless fishes (n=353) show a rapid shift to deeper waters

following nearshore origination. Full distributions shown in Figs. S21 and S22 and Additional Data File S1.

Supplementary Materials

Materials and Methods

Supplementary Text

References (29-60)

Tables S1-S3

Figures S1-S23

Additional Data Tables S1-S3

Database S1 (doi:10.5061/dryad.g08m87q)

Supplementary Materials for

The Nearshore Cradle of Early Vertebrate Diversification

Lauren Sallan, Matt Friedman, Robert S. Sansom, Charlotte M. Bird, Ivan J. Sansom

correspondence to: lsallan@upenn.edu, i.j.sansom@bham.ac.uk

This PDF file includes:

Other Supplementary Materials for this manuscript includes the following:

Additional Data Files S1-S3 as zipped archives: Mid-Paleozoic Gnathostome Occurrences; Mid-Paleozoic Habitat Distributions; Statistical Comparison
Database S1 as a zipped archive on Dryad (doi:10.5061/dryad.g08m87q)

Materials and Methods

Databasing of Early Vertebrate Occurrences and Habitats.

We manually compiled occurrences and environmental data from the early record of total-group gnathostomes (jawed vertebrates and their jawless relatives) in order to reconstruct habitat preferences around the origins of major clades. Taxa and locality information were assembled from available taxonomic and faunal literature for the mid-Paleozoic (Ordovician-Devonian; 488-359 Mya)(*29*)(Additional Data File S1); previously compiled and publicly available databases are notably incomplete for these clades and time periods (*4*). We focused our compilation efforts on three main areas relevant to our hypotheses: 1) occurrences from the oldest five localities and other strata of equivalent age for major gnathostome clades. 2) all occurrences for jawless gnathostomes with genus or family-level phylogenetic placement, 3) later jawed gnathostomes up to the end-Devonian. The first two sets were optimized for use with ancestral state reconstruction, while the last was included in our statistical analyses of habitat distributions. These occurrences and their specific references and sources are documented in Additional Data File S1.

We used the primary sedimentological, geochemical and the fossil invertebrate community literature, environmental information for specific horizons in the Paleobiology Database (PBDB)(*14*), and Benthic Assemblage (BA) zone assignments in Boucot and Lawson (*10*) to assign our assembled vertebrate occurrences to BA zones as used by Boucot (*30*)(Fig. 1, Additional Data File S1), based on the most unit or horizon-specific information available. As explained in text, Benthic Assemblage zones represent habitats along a marine depth gradient, ranging from BA1 (shoreline, intertidal, marginal marine) to BA6 (open water, basin; *30*). We followed Plotnick (*31*) in the addition of BA0 to represent freshwater localities (e.g. lacustrine, fluvial). Occurrences could fall into more than one BA zone if: 1) a species was recovered from a wide habitat range at that locality; 2) there was uncertainty about the exact environment of the horizon within the wider habitat range represented by the formation; 3) there was evidence of mixing between zones (e.g. marine incursions into freshwater or estuarine habitats; leading to BA 0-1) and it was not clear where the species lived); 4) the horizon or formation represents a broad range of zones with some existing uncertainty as to the actual environment. Habitat uncertainty, as captured by options 2-4, was parsed into more and less likely environments based on external data (not assumed preferences for species), with less likely residence indicated by question marks in our data files (Additional Data File S1). Zone assignments were made independent of the vertebrate fauna.

For occurrences to be used in phylogenetic comparative analyses (sets 1 and 2), we assigned maximum and minimum ages for the shortest unit of geological time (e.g. conodont zone, regional stage) and/or lithology (e.g. horizon, formation) associated with each gnathostome occurrence. All chronostratigraphic dates were obtained from regional substage and index fossil zone correlations in the Geological Timescale 2012 (*29*) for consistency. References for specific papers and collections used in age assignments are listed in Additional Data File S1. We also translated any Benthic Assemblage zone uncertainty into a distribution of probability of occurrence in each zone for use with our phylogenetic comparative methods. For example, an occurrence likely but not certain to fall entirely within BA3 would be listed as ‘2?-3-4?’ in our raw data, and assigned prior

probabilities of BA2: 0.25, BA3: 0.5, and BA4: 0.25. See Database S1 for these input files.

Ancestral State Reconstruction.

We constructed consensus trees for early gnathostomes using the program *Mesquite* (*32*), with branching patterns based on recent published topologies (see below). Our terminal taxa consisted of species-level occurrences from our new compendium (Figs. S1-S10, Additional Data File S1, Database S1). Multiple occurrences for species or genera were placed in polytomies so as not to unnecessarily bias the analysis towards first occurrences, although early occurrences with shorter branches should have a larger effect on the ancestral state. We assembled four versions of the total-group gnathostome tree to accommodate uncertainty surrounding the paraphyly or monophyly of "placoderms" and an Ordovician or Silurian first occurrence for definitive total-group chondrichthyans. Topologies were based on Sansom et al. 2010, Zhu et al. 2013, and Keating and Donoghue 2016 (gnathostome relationships; *33-35*), Lu et al. 2017 (placoderm paraphyly; *36*); King et al., 2017 (placoderm monophyly; *37*), and Andreev et al. 2017 (chondrichthyan relationships; *15*), Sansom et al. 2008, Sansom, 2009a, Sansom 2009b (osteostracans; *27, 38, 39*); Wilson and Marss 2009 (thelodonts; *40*), Randle and Sansom 2017 (heterostracans; *41*); Gai and Zhu 2007 (galeaspids; *42*); Blom 2012 and Keating and Donoghue 2016 (anaspids; *35, 43*). All four gnathostome trees contained occurrences for all phylogenetically-constrained taxa, and their taxonomically-close relatives, from the five oldest localities (based on maximum ages) for each clade, as well as occurrences from other sites with overlapping age ranges (Figs. S2-S5). Nexus files containing these topologies are available in Database S1.

We applied Bayesian phylogenetic methods to reconstruct ancestral Benthic Assemblage zones for early total-group gnathostomes. This uses an iterative modelling approach that takes into account branch lengths and empirical data in the form of observed probabilities of residence in each Benthic Assemblage zone for the terminal taxa (*13*). We did the same for jawless vertebrate clades representing the major axis of early gnathostome body plans (macromeric: heterostracans, galeaspids, osteostracans, vs. micromeric: thelodonts, anaspids). We additionally compiled occurrence data for Ordovician-Devonian 'complex' conodont taxa (Euconodonta), themselves flexible and scaleless like our micromeric set, using an available phylogenetic framework in order to test for potential bias in the methods independent of observed distributions (*44*). Complex conodonts can serve as a comparison in phylogenetic analyses, as they are total-group or crown-group vertebrates, have similar hard tissues, are globally and densely-sampled (Fig. 1B, figs. S14, S15, S23) and have a consistent presence in deeper water (see below). Complex conodont early occurrences are found in Additional Data File S1.

We also constructed clade-level trees containing all environmentally-resolved occurrences for phylogenetically-resolved taxa and their close relatives in five major jawless gnathostome clades (osteostracans, galeaspids, heterostracans and their Ordovician-age sister clades, anaspids, and thelodonts, see above for references) with divergent body plans and origination and extinction in the mid-Paleozoic (Figs. S6-S10) Finally, we used the complex conodont phylogeny by Donoghue et al. 2008 (*44*) alongside the earliest occurrences (oldest locality and sites with overlapping potential age

ranges) for same comparative reasons laid out above (Fig. S23). Nexus files containing these topologies are available in Database S1.

In order to generate branch-durations for our analyses, we assigned each sampled locality a single random date within the potential age range set by our maximum and minimum stratigraphic ages. These dates were applied to all terminal taxa from that site or fauna. We then performed timescaling using the "equal" method in the *date.phylo* function, now available in the R package *strap* as *DatePhylo,* with the root age set to 1 million years as a default (*45, 46*). Tip ages are available in Database S1. To reconstruct ancestral states, we used the Bayesian function *AncThresh* in the R package *Phytools* (*47*). AncThresh is a function which uses a threshold model (*13*) to reconstruct the ancestral states of discrete, ordered traits. This fits the purposes and aims of our study: Benthic Assemblage zones are already ordered from 0 to 6 along the depth gradient (Fig. 1).

In the model as implemented in *AncThresh*, an unobserved continuous trait called "liability" changes value along the branches of a tree according to a Brownian Motion (BM), Ornstein-Uhlenbeck (OU) and Pagel's *lambda* model (*13*). Transitions between ordered, discrete states are linked to specific values for liability, or threshold parameters, which are estimated from sampled states for terminals and can be interpreted as the cost or amount of evolutionary change required (*13*). Here, we assume liability represents as continuous changes in traits which permit movement between Benthic Assemblage zones, including shifts in home range, dispersal ability, physiology, behavior, form and other traits linked to mobility along the depth gradient. The thresholds then represent the amount of total change necessary to shift into the next Benthic Assemblage zone. We assigned prior probabilities for the presence of each terminal taxon occurrence in each Benthic Assemblage zone based on the environmental data for localities. These input files are available in Database S1.

We implemented all three models in *AncThresh* as these represent different processes of habitat dispersal. Brownian motion implies random dispersal along branches, with an equal probability of moving outward and returning to ancestral states and diffusion of a clade through trait space over time (*13*). Ornstein-Uhlenbeck (OU)(*48, 49*) adds a tendency to return to a preferred habitat within a set interval represented by the parameter *alpha*. When using a time-scaled phylogeny, as here, mean *alpha* can be used to estimate the usual time until return to the mean value, or habitat of preference (phylogenetic half-life; ln(2)/*alpha)*(Tables S1-S3)(*16*). The strength of *alpha* could be linked to selection on dispersal or habitat-linked traits, such as armor or swimming ability. Pagel's *lambda (50)* is a modification of Brownian Motion that transforms branch lengths to estimate phylogenetic signal. Here, it estimates the tendency of habitat distributions at the tips to be wholly dependent on ancestry or shifts along underlying branches (lambda=1, or BM) or completely independent of it (lambda=0).

We ran each model for 1 million generations with the first 20% excluded as "burn-in." We applied the Deviance Information Criterion (DIC) (*51*) as implemented in *Phytools* (*47*) to select the best fit and examined the parameters (thresholds, *alpha*) to determine convergence, and converted these to DIC weights using the procedure for Akaike weights (*52*). We then reran the best-fit model for 20 million generations if the parameters generated for the raw occurrences were consistent (e.g. normally distributed in the case of *alpha*) and 50 million if not.

Finally, to counteract environmental sampling uncertainty within vertebrates alone, we increased the minimum prior probabilities of terminal taxon occurrence in each Benthic Assemblage zone to 5% and 10%. We then reran all our analyses in *AncThresh* with these flattened distributions of priors. This increased the probability of unsampled existence throughout the habitat range and thus decreased the significance of recorded occurrences, generating conservative estimates for ancestral states and dispersal. Results of our analyses were plotted in Figures 1-3, S2-S10, and S23 using the function *geoscalePhylo* in the R package *strap* (*45*). All input files, R code, and results are found in Database S1 on Dryad.

Sampling Controls.

We surveyed available, global mid-Paleozoic datasets containing similar environmental data to test whether our ancestral states were influenced by global preservational or sampling bias, such as rock volumes. These could be not directly informative for our priors given differences in data collection aims, coverage, and environmental binning, as well as real habitat differences among clades which influence distributions (e.g. common cause hypotheses)(*25*). That said several environmental distribution datasets were used within statistical comparisons of environmental distributions to 1) reveal potential megabiases and 2) test the significance of gnathostome ancestral habitats as revealed by phylogenetic comparative methods.

To establish a baseline environmental distribution in the mid-Paleozoic, we downloaded global strata (n=3347), genera (n=24211) and occurrence records (n=111364) from the Paleobiology Database (PBDB)(*14*) using default settings sampling in bins. We binned these by stage and environment along the depth gradient (Figs. 1B, S11, S12; Additional Data File S2; Database S1). The PBDB is an independent resource; it remains extremely undersampled for early vertebrates (*4*) and lacks most of the occurrences and localities in our gnathostome dataset. However, it is more robust for the invertebrate record and fossiliferous rocks as a whole. The PBDB's coarse environmental assignments are roughly equivalent to Boucot's (*30*) Benthic Assemblage zones in shallow waters (fluvial+lacustrine=BA0; marginal marine=BA1; shallow subtidal=BA2). Deeper water bins were less defined in terms of communities and position along the depth gradient. We determined these to be equivalent to overlapping ranges of Benthic Assemblage zones (deep subtidal=BA3-4; reef=BA3-4; offshore=BA4-5; basin/slope=BA5-6). In addition, freshwater records are largely missing from the Ordovician-early Devonian, during intervals when gnathostomes inhabited such settings. These environmental differences do not allow us to directly compare BA zone distributions in the PBDB and with our own gnathostome dataset. However, they do permit other comparisons (e.g. BA1, 2, and 3-6) which would reveal differences in nearshore or offshore distributions (Fig. S11, S13, S15; Additional Data File S3).

To establish a baseline for preservation potential and vertebrate tissue sampling across the depth gradient, we downloaded the subset of mid-Paleozoic microfossil conodont occurrences (n=11915) and genera (N=1308) in the PBDB, binned again by environment and stage (Figs. 1B, S14; Additional Data File S2; Database S1). The calcium-carbonate heavy benthic invertebrate fossils that make up a majority of PBDB records are both materially and taphonomically-distinct from hydroxyapatite-bearing gnathostomes (*17*). Conodonts are the likely sister group of cyclostomes, gnathostomes

or crown vertebrates as a whole (*4*) and bear elements with hydroxyapatite materials convergent on dentin and enamel. As index fossils, conodonts are globally widespread and densely-sampled within the PBDB, and have a consistent presence in deep and shallow water from the early Ordovician (Fig. S14; Additional Data File S2; Database S1)(*4*). However, the phylogeny, taxonomy and record of conodonts is too unresolved to fully determine ancestral distributions at this point in time; their origins are likely Cambrian in age (*4*). Instead, we used PBDB conodont records as a proxy distribution for vertebrate remains under similar sampling and data collection aims as the PBDB as a whole. This allows comparisons of environmental distributions within a single dataset.

To establish a separate baseline distribution of sampling across all marine Benthic Assemblage zones without binning uncertainty present in the PBDB, we compiled environmental and stage data for the primarily invertebrate Silurian and Lochkovian regional paleocommunities described in Boucot and Lawson (n=2401)(*10*)(Fig. S13, Additional Data File S2; Database S1). Boucot and Lawson's primarily Silurian and Lochkovian paleocommunity survey (*10*) was assembled separately from the PBDB. It has not been fully incorporated into the public database, presumably due to a mismatch in scope and aims. While assemblages are not directly comparable to occurrences or strata, Boucot and Lawson's efforts are more standardized than the PBDB. Paleocommunities are erected on the basis of common assemblages named for key, often shared, marine invertebrate taxa. The survey consists of assignment of these communities within different regions and formations into specific Benthic Assemblage zones, and likely required a minimum level of abundance or collection effort for identification. While the survey contains a few vertebrate chapters, and vertebrates are resident at some communities, these have been excluded from consideration here. Paleocommunities with wide environmental ranges or uncertainty were counted in multiple zones as a conservative estimate (Fig. 1B, fig. S13; Additional Data File S2).

Finally, we binned our assembled gnathostome occurrences by stage and Benthic Assemblage zone within the entire mid-Paleozoic (n=2827)(Figs. 1B, 1C, 2, 3, S1, S16-S18; Additional Data File S2). We augmented our ancestral state analysis datasets, which contained all occurrences for phylogenetically-constrained jawless fishes and early members of jawed fish clades (see above), with less constrained occurrences for later jawed fishes in the Devonian (Additional Data File S2). As with Boucot and Lawson's paleocommunities, gnathostome occurrences with uncertainty or wide range in environment or age were binned in multiple Benthic Assemblage zones or stages, presenting a more conservative estimate than for our prior probabilities. To check our ancestral state results and perform statistical comparisons, our total-group gnathostome dataset was subsampled into provide separate distributions for jawed (n=1343) and jawless fishes (n=1484), micromeric (n=353) and macromeric (n=1123) clades, early vs. later occurrences for all groups (based on the ancestral state dataset), Marine occurrences (n=2147) for comparison with the Paleobiology Database and to control for later freshwater invasion, and Silurian and Lochkovian marine occurrences (n=1035) for comparison with Boucot and Lawson (Figs. 1B, 1C, 2D, 3C, S1, S11-S22).

The original PBDB .csv files and paleocommunity information from Boucot and Lawson (1999; *10*) are available in Database S1 on Dryad. Counts and proportions by stage and bin for strata, richness, occurrences and paleocommunities, and summary distributions, are collected in Additional Data File S2.

Statistical Tests of Distributions.

After assembling our habitat distribution datasets as described above, we first visualized the habitat range within each stage using a matrix of binned datapoints (Additional Data File S2). We then calculated the percentage of datapoints in each habitat both across the mid-Paleozoic and in each stage, and generated histograms representing these proportional distributions (Figs. 1B, 1C, 2D, 3C, S16-S22; Additional Data File S2). We also generated histograms for subsets involving only marine BA zones (as conodonts do not have freshwater occurrences), and marine habitats in the Silurian and Lochkovian, as Boucot and Lawson (*10*) focus on that interval (Additional Data File S2). These plots allowed us to visually assess differences and gaps in habitat distributions which might be indicative of megabiases, both between fossil record metrics and datasets, and across time (Figs. 1B, 1C, S1, S11-S22).

We designed our statistical tests in R to quantify observed differences or similarities in the habitat distributions. Appropriate statistical methods were limited as the data are categorical, consisting of counts within discrete bins (e.g. contingency tables), have differences in habitat binning (e.g. the shared Benthic Assemblage zones of some PBDB environmental bins such as "offshore"; see above) and temporal ranges, come from independent sources and/or capture different independent variables. Thus, we could not apply typical tests of distributions which depend on the use of means, or similar values and populations, such as non-parametric rank-order tests like Mann-Whitney U. We used linear regressions for comparisons between datasets and variables (e.g. conodont vs gnathostome communities). This involved adjustments in habitat binning and temporal ranges to make these sets comparable. Reduction in bins limited the power of some comparisons, especially between sets using Benthic Assemblage zones (e.g. our vertebrate data, Boucot and Lawson's paleocommunities) and PBDB records, as BA3-6 records had to be pooled into the single category "deeper" given overlap in PBDB environmental binning (see above)(Figs. S12, S13, S16). We used Pearson's Chi-squared tests to compare subsets of the same data (e.g. conodont occurrences vs. other PBDB occurrences)(Figs. S15, S18). For all tests, we generated bar graphs of the distributions in each comparator set to understand the results. The input data, R code, and results for these tests are available in Additional Data File 3 and Database S1 on Dryad.

To test for potential global sampling biases in the mid-Paleozoic, we used linear regression to test the strength of the relationship between the overall distributions of fossiliferous strata in the Paleobiology Database and occurrences, and strata and richness, in marine settings, and in marine settings during the Silurian and Lochkovian (Figs. 1B, S12; Additional Data File S3; Database S1). Next, we used a linear regression to test for correlation between Silurian and Lochkovian Paleobiology Database occurrence distributions in BA1, 2, and pooled deeper zones (BA3-6) with the distribution of Boucot and Lawson's paleocommunities, which are also related to abundance (Fig. S13; Databases S3, S4). We used Pearson's Chi-squared test to for differences between PBDB conodont occurrences or richness and those for all other marine Paleobiology Database taxa, using both the entire mid-Paleozoic record and a subset focused on the Silurian and Lochkovian (Fig. S15; Additional Data File S3; Database S1).

Next, we tested whether distributions in the previous existing datasets explained our gnathostome distributions. We used linear regression to test for correlation between

Boucot and Lawson's paleocommunities (*10*) and Silurian and Lochkovian marine gnathostome occurrences, as these are both binned by exact BA zone (Fig. S16; Database S3). We used linear regressions to test for correlation between marine PBDB occurrences and gnathostome occurrences in the mid-Paleozoic and Silurian and Lochkovian, again binning datapoints by BA 1, BA2 and "Deeper" (BA 3-6) to account for environmental bin differences (Fig. S16; Additional Data File S3; Database S1). This would account for global bias in sampling intensity or fossilization. Finally, we used linear regressions to test for correlations between PBDB conodont occurrences and marine gnathostome occurrences in the mid-Paleozoic and Silurian and Lochkovian (Fig. S16; Additional Data File S3; Database S1). This would show if preservational similarity and potential primarily explained gnathostome distributions.

In addition to the above tests, we also used Pearson's Chi-squared test to determine if early occurrences for major gnathostome groups (total group gnathostomes; jawed fishes; jawless fishes; macromeric jawless fishes; micromeric jawless fishes) were significantly shallower marine than later occurrences independent of time (Figs. S18, S20, S22; Additional Data Files S1, S3; Database S1). This would show whether our ancestral state results were attributable to changes in preservation potential over the mid-Paleozoic, or whether they resulted from persistent environmental restriction in origination.

Supplementary Text

Fossil Record Summaries for Mid-Paleozoic Vertebrates

Total-Group Gnathostomes. Vertebrates are divided in to two main groups: those that form the modern jawless agnathans or cyclostomes (hagfish and lampreys) which are considered to be monophyletic; the extant jawed gnathostomes and the fossil components that comprise the gnathostome total-group and record their evolutionary trajectory away from a shared common ancestor with the cyclostomes (*4, 8, 17*). Vertebrates as a group have their first appearance in the Cambrian Chengjiang fossil-lagerstätte (*53*). The cyclostome fossil record is dominated by conodonts (see section below) with sporadic appearance of unarmored forms in localized lagerstätte. The gnathostome total-group (including the extinct jawless anaspids, thelodonts, heterostracans, galeaspids and osteostracans and jawed placoderms that comprise the gnathostome stem-group) have a considerably richer record, largely as a result of their more extensive biomineralization and hence increased preservation potential.

Jawed Gnathostomes. Vertebrates with jaws (otherwise termed 'mandibulate gnathostomes' (*8*)) dominate the diversity of living vertebrates, comprising over 99% of the extant members of the group. In the middle Paleozoic, the jawed gnathostomes include the extinct placoderms (Silurian–Devonian), the chondrichthyans (Ordovician–present) and the osteichthyans (Silurian – present)(*8*). Their first appearance in the fossil record is contentious, with indications from dermal scale remains that representatives of the chondrichthyans have their first appearance in the Upper Ordovician (Sandbian)(*54*) or earlier in the Middle Ordovician (Darriwilian)(*55*) but they remain a comparatively limited component of the vertebrate faunas until undergoing a series of major radiations in the late Silurian and Devonian. After their initial appearance, all major groups of jawed

gnathostomes have a record that suggests they achieve a cosmopolitan distribution through the Silurian and Devonian, and, concomitantly, a widespread dispersal across the marine shelf into deep waters whilst also invading estuarine and freshwater environments (Fig. S1)(*4, 8, 17*).

Heterostracans. The Heterostraci traditionally encompass the two major groups, the Pteraspidiformes and the Cythaspidiformes, together with a number of more loosely allied taxa such as the stratigraphically oldest heterostracan *Athenaegis* from the Llandovery, Lower Silurian of Canada (Additional Data File S1). However, a recent phylogenetic treatment by Randle and Sansom, 2017 (*41*) has found the latter to be paraphyletic with respect to the former; we follow this topology here. All members of the Heterostraci *sensu stricto* possess a paired single external branchial opening, dorsal and ventral headshields that consist of acellular aspidin surmounted by tubular dentine and a single crystalline enameloid cap (*17*). The relationship between heterostracans and Ordovician astraspids and arandaspids is more problematic due to the absence of a number of heterostracan synapomorphies (notably the single external branchial opening), although the Ordovician taxa are often expressed as immediate sister groups with respect to the Heterostraci *sensu stricto* (*4, 8, 17*). Thus, we include a polytomous sister group of Ordovician forms in our analysis of this clade (Figs. 2A, S6, S19A; Database S1).

The habitat occurrence data for heterostracans and their close relatives show several distinct patterns with a temporal component (Additional Data File S1). Arandaspids and astraspids are found exclusively in nearshore Ordovician sediments, centered on the tidal and subtidal zones (Fig. S16). In contrast, the earliest heterostracan, *Athenaegis,* is found on the shoreward end of a reefal setting, which our analysis suggests is an anomalous occurrence (Additional Data File S1). This appearance presages a major split in both the phylogeny of heterostracans and their habitat preferences. One segment of heterostracan diversity, the paraphyletic Cyathaspidiformes (*41*), first appear on the backreef and are preferentially found in reefal and deep lagoonal environments early, while the widespread, relatively robust and flattened genera *Poraspis* and *Vernonaspis* and some other late occurring forms shifted back to shore and freshwaters. In contrast, the other monophyletic division, the Pteraspidiformes (*41*), stay in the shallows and move into freshwater early, while a few later, streamlined lineages (including the *Rhinopteraspis*) make it to the shelf and open ocean (Figs. 2A, S6; Additional Data File S1).

Galeaspids. Galeaspids are jawless vertebrates that are thought to be endemic to the Siluro-Devonian of China and northern Vietnam, with first appearances in the Llandovery, Lower Silurian of Tarim and South China (Additional Data File S1). These 'basal' galeaspids constitute a sister group to the more derived Eugaleaspidiformes, Polybranchiaspidiformes and Huananaspidiformes (*26*). Significant morphological features include a large anterior opening (hypophyseal) in the medio-dorsal headshield (*56*); the headshield being a massive construction with endo- and exoskeletal contributions. The absence of paired fins has consistently placed galeaspids as basal to the osteostracans in the derived gnathostome stem-group (*4, 8, 35*).

Like similarly robust and flattened osteostracans, most galeaspids are found mostly in shallow waters early on in their existence and likely originated near the

shoreline (Figs. 2B, S7, S19B; Additional Data Files S1, S2). However, they do show a tendency to move into deeper and freshwaters later in their temporal range, with *Tridentaspis, Duyunolepis* and related genera found on the reef and beyond (Figs. 2B, S7, S19B; Additional Data Files S1, S2). Two relatively early lineages, *Geraspis* and *Hanyangaspis,* have been recovered from open water localities late in their temporal ranges (Additional Data File S1). However, as evidenced by earlier occurrences of these same genera and their sister taxa in very shallow waters, this may represent postmortem transport.

Osteostracans. Osteostraci is a crownward component of the gnathostome stem-group, with a first appearance in the middle of the Silurian (Wenlock) and last appearance in the Late Devonian, before the Frasnian-Famennian Kellwasser extinction event (Figs. S1, S8, S19C)(*4, 8, 17*). The basic form of osteostracans is in line with many jawed gnathostomes of the same Silurian-Devonian interval, such as various groups of placoderms. The 'ostracoderms,' such as the Osteostraci, were hypothesized to show strong endemism following their first appearance and subsequent diversity that is influenced by sea-level change (*6*).

Osteostracans are primarily restricted to shallow environments: there are no known occurrences in deep water facies and they underwent at least two phylogenetically independent transitions from marine/brackish Silurian environments to fluvial Devonian facies (Figs. 2C, 2D, S19C; Additional Data Files S1, S2). This significant restriction in habitat appears to underpin osteostracan paleogeographic range, which is essentially limited to Laurussia/Euramerica (the Old Red Sandstone continent) during the Silurian and Early Devonian save a couple of isolated genera in the distant peri-Siberian terranes (*27, 38, 39*).

Thelodonts. Thelodonti is largely known from isolated scales that are common components of the vertebrate record from the late Ordovician (*28, 54, 57*) through to the Late Devonian (middle Famennian; *28*)(Figs. 3A, S9, S21A; Additional Data File S1). These micromeric scales covered the body of jawless fish that variously exhibited deep and shallow bodies, with and without paired pectoral flaps (*17*). Thelodonts are one of a number of micromeric taxa that exhibit rapid dispersal following their origination (*24*).

The habitat occurrence data for thelodonts, in contrast to macromeric taxa, exhibit a complex pattern where several low-level lineages shifts to deeper and shallower waters, (Figs. 3C, S9, S21A) although many early members of Thelodonti are excluded from the Wilson and Märss, 2009 (*40*) scheme due to limited morphological data. Nevertheless, expansion away from shallow marine habitats is achieved separately in the fork-tailed and deep bodied Furcacaudiformes and the more disparate Thelodontiformes (Fig. 3A). Thelodont habitat dispersal is also reflected in their paleogeographic occurrence. They first appear in the Sandbian of Laurentia (*54*) and undergo rapid range expansion thereafter (*28*). At present, too little is known about the stratigraphically oldest thelodonts (the Sandiviformes *sensu 28*) to include anything more than a single species within the phylogenetic analysis. The appearance of *Stroiniolepis maenniki* (from the Upper Ordovician of the Russian Federation) nested within, but not basal to, the Thelodontiformes points toward substantial ghost ranges within the thelodonts (Fig. 3A, S9; Additional Data File S1; Database S1).

Anaspids. The Anaspida are a comparatively low diversity group that in recent phylogenetic treatments resolve as two clades, the naked anaspids (*Jamoytius* and *Euphanerops*) and a weakly armored group that is largely comprised of the birkeniids (Figs. 3B, S10, S21B). Their stratigraphic and geographic range is predominately Silurian of North America and Europe, although well characterised naked anaspids are described from the Late Devonian (the Miguasha lagerstatte of Quebec)(Additional Data File S1), and a '*Jamoytius*-like' form in the Soom Shale of South Africa (*58*) may represent an Ordovician record, but this has yet to be formally described. The phylogenetic position of the anaspids has been contentious, with conflicting hypotheses placing them as stem-lampreys, the most plesiomorphic of the stem-gnathostomes or embedded at various positions within the 'ostracoderm' component of the stem-gnathostomes including as the immediate sister-group to the jawed vertebrates (*4, 17*). In their most recent treatment, Keating and Donoghue 2016 (*35*) resolve them as a monophyletic clade nested among the stem-gnathostomes between the heterostracans and the galeaspids.

Like the similarly micromeric thelodonts, our analysis suggests most scaled anaspids originated in deeper subtidal zones, as most remains have been found there and diversification appears to have been rapid (Figs. 3B, S10, S21B). However, many early examples come from recovered from shallow and freshwater localities in numbers near equal to similarly aged occurrences on the backreef and shelf (Fig. S12B; Additional Data File S1). This suggests that armored anaspids themselves may have dispersed quickly after their origin. In contrast, naked anaspids are found only in freshwater and estuarine settings throughout their entire temporal range (Figs. 3B, S10, S21B; Additional Data File S1).

Conodonts. Conodonts are a diverse group of stem-group cyclostomes whose fossil record is dominated by their mineralized feeding apparatus (the tissues of which are convergent on gnathostome biomineralization (*59*). They have a first appearance in Cambrian, undergo a rapid dispersal in the marine realm to occupy a wide range of water depths and develop a cosmopolitan distribution before their decline and ultimate extinction in the end-Triassic (*4*). Knowledge of the body plan of conodonts remains restricted to a small number of taxa preserved in the Soom Shale (Upper Ordovician, South Africa) and Granton Shrimp Bed (Carboniferous, Mississippian, of Scotland)(*4, 17*).

The 'complex' conodonts used in phylogenetic analyses include a wide variety of taxa that have an intricate multi-function feeding apparatuses and are thought to have occupied a wide range of ecological niches ranging from extremely shallow (peritidal) to deep open water settings (Figs. S14, S23; Additional Data File S2; Database S1). Interpretations of their paleoecology are hampered by taphonomic biases against the preservation of their soft parts, although recent work indicates that at least some 'complex' conodont species existed as pelagic organisms distributed in a depth tiered fashion (*60*).

Fig. S1.

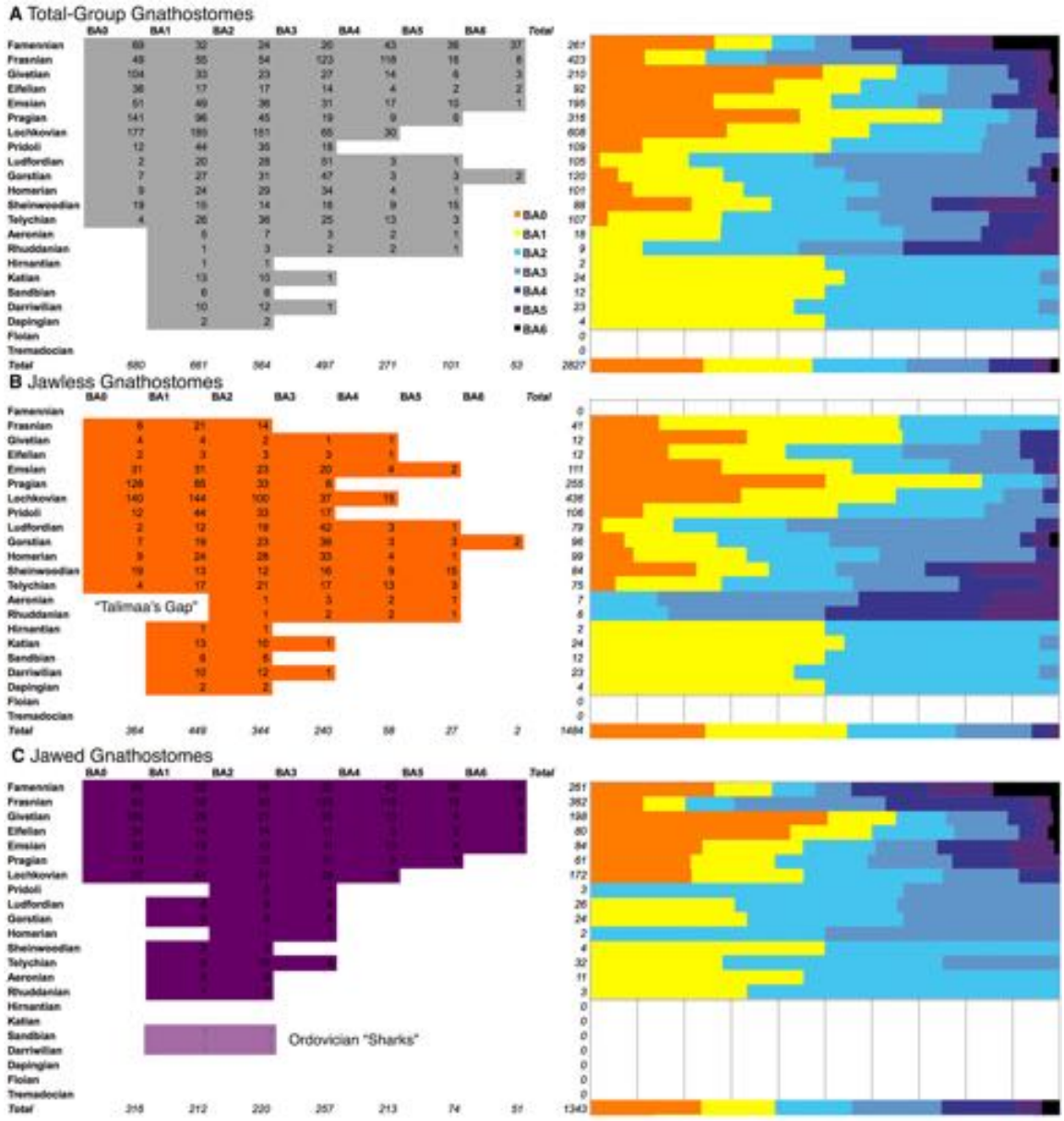

Benthic Assemblage (BA) Zone Distributions for Total-Group Gnathostomes During the Ordovician-Devonian. A-C) Distributions of occurrences by environment for A) Total-group Gnathostomes B) Jawless Gnathostomes and C) Jawed Gnathostomes. Matrices on the left shows range of occurrences by stage. Histograms on the right show the proportion of occurrences in each Benthic Assemblage zone. The early Silurian gap in sampling of jawless fishes in BA0-1 (B) corresponds to "Talimaa's Gap" (*4*); occurrences of jawed fishes and other jawless forms are likewise rare. Ordovician "chondrichthyans" (sharks) in C are shown as transparent and not represented in totals, as these were only used in supplementary phylogenetic analyses including these disputed Ordovician taxa (Figs. S4, S5). The same BA1-2 occurrences are also assigned to jawless fishes in statistical analyses, in line with our main phylogenetic analyses assuming a Silurian first

appearance for jawed fishes (Figs. 1, S2). Detailed records available in Additional Data File S1. Exact counts in each bin available in Additional Data File S2

Fig. S2

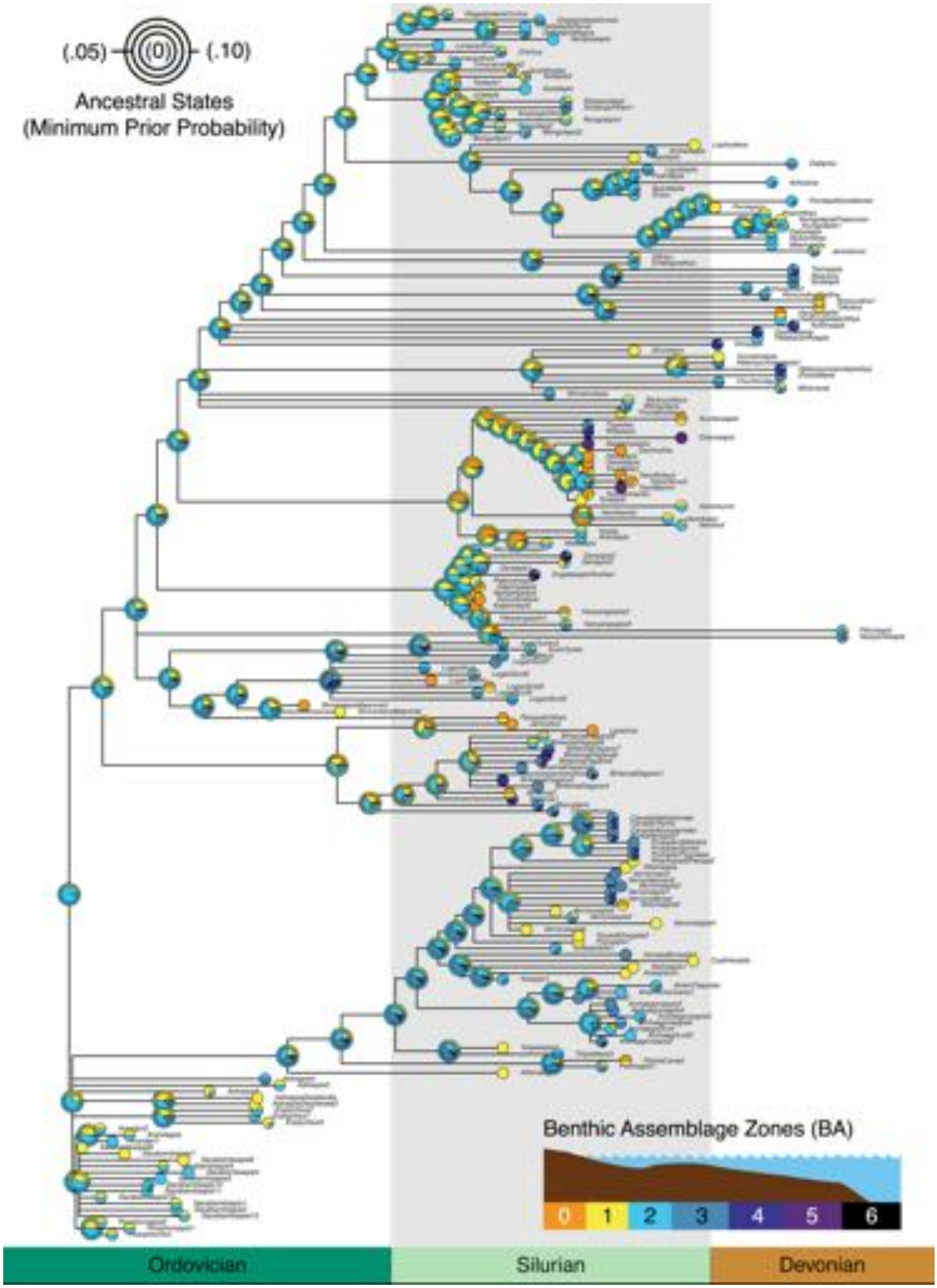
(.05)
(0)
(.10)
Ancestral States
(Minimum Prior Probability)
Benthic Assemblage Zones (BA)
0
1
2
3
4
5
6
Ordovician
Silurian
Devonian

Ancestral Habitats for Early Total-group Gnathostomes Under a Silurian First Appearance for Jawed Fishes and Placoderm Paraphyly, Nested ancestral states represent estimations from taxon distributions with three different levels of minimum prior probability of occurrence in any bin: 0 (center, representing raw data), 0.05 (middle ring, representing moderate sampling uncertainty) and 0.10 (outer ring, representing greater sampling uncertainty). Benthic Assemblage key given in figure. Phylogeny based on references given in methods section. See Additional Data File S1 for tip occurrence details and Database S1 for input files, phylogenies, R code, tip ages, and all results.

Fig. S3

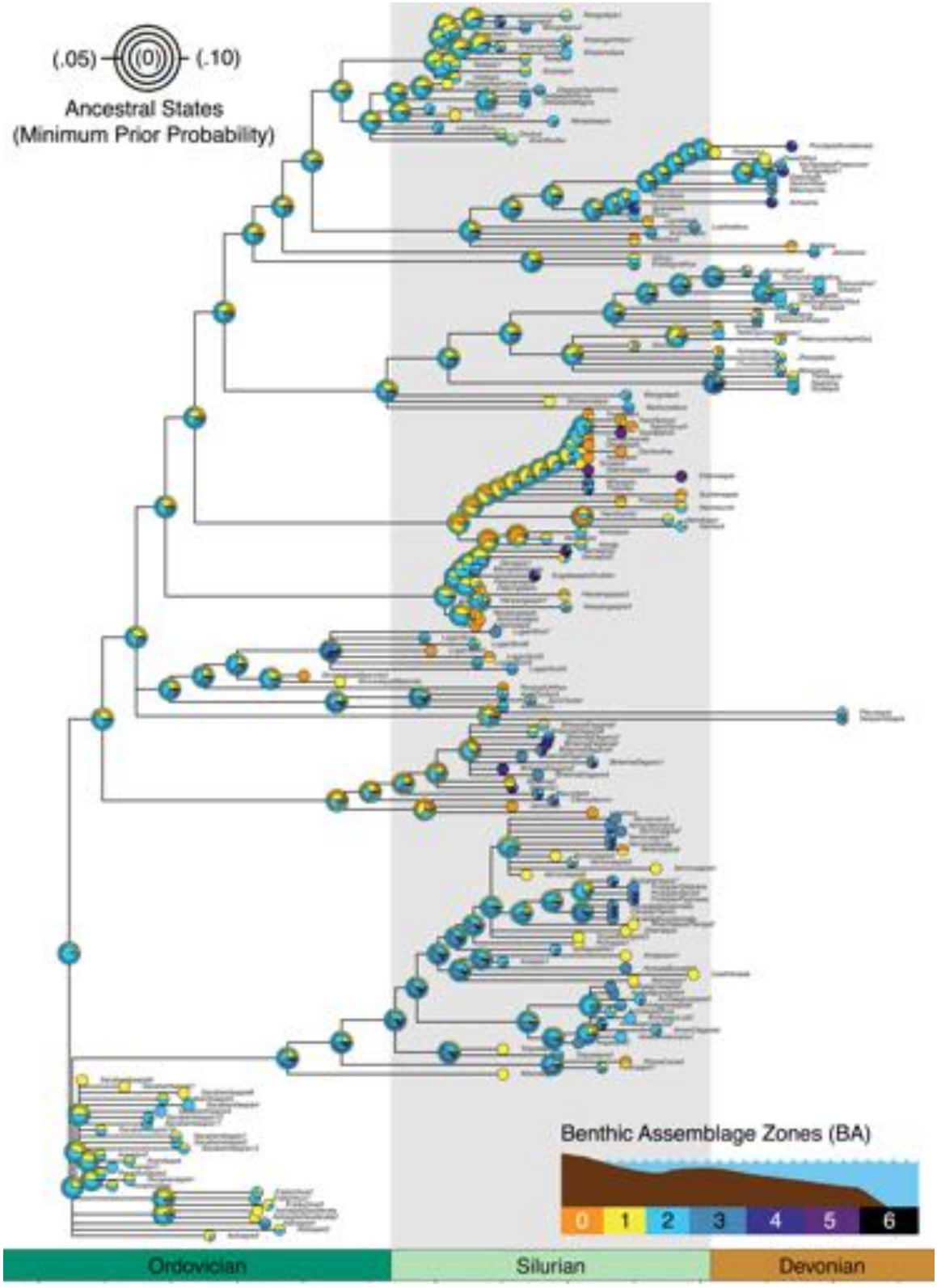
(.05)
(0)
(.10)
Ancestral States
(Minimum Prior Probability)
Benthic Assemblage Zones (BA)
0
1
2
3
4
5
6
Ordovician
Silurian
Devonian

Ancestral Habitats for Early Total-group Gnathostomes Under a Silurian First Appearance for Jawed Fishes and Placoderm Monophyly, Nested ancestral states represent estimations from taxon distributions with three different levels of minimum prior probability of occurrence in any bin: 0 (center, representing raw data), 0.05 (middle ring, representing moderate sampling uncertainty) and 0.10 (outer ring, representing greater sampling uncertainty). Benthic Assemblage zone key given in figure. Phylogeny based on references given in methods section. See Additional Data File S1 for tip occurrence details and Database S1 for input files, phylogenies, R code, tip ages, and all results.

Fig. S4

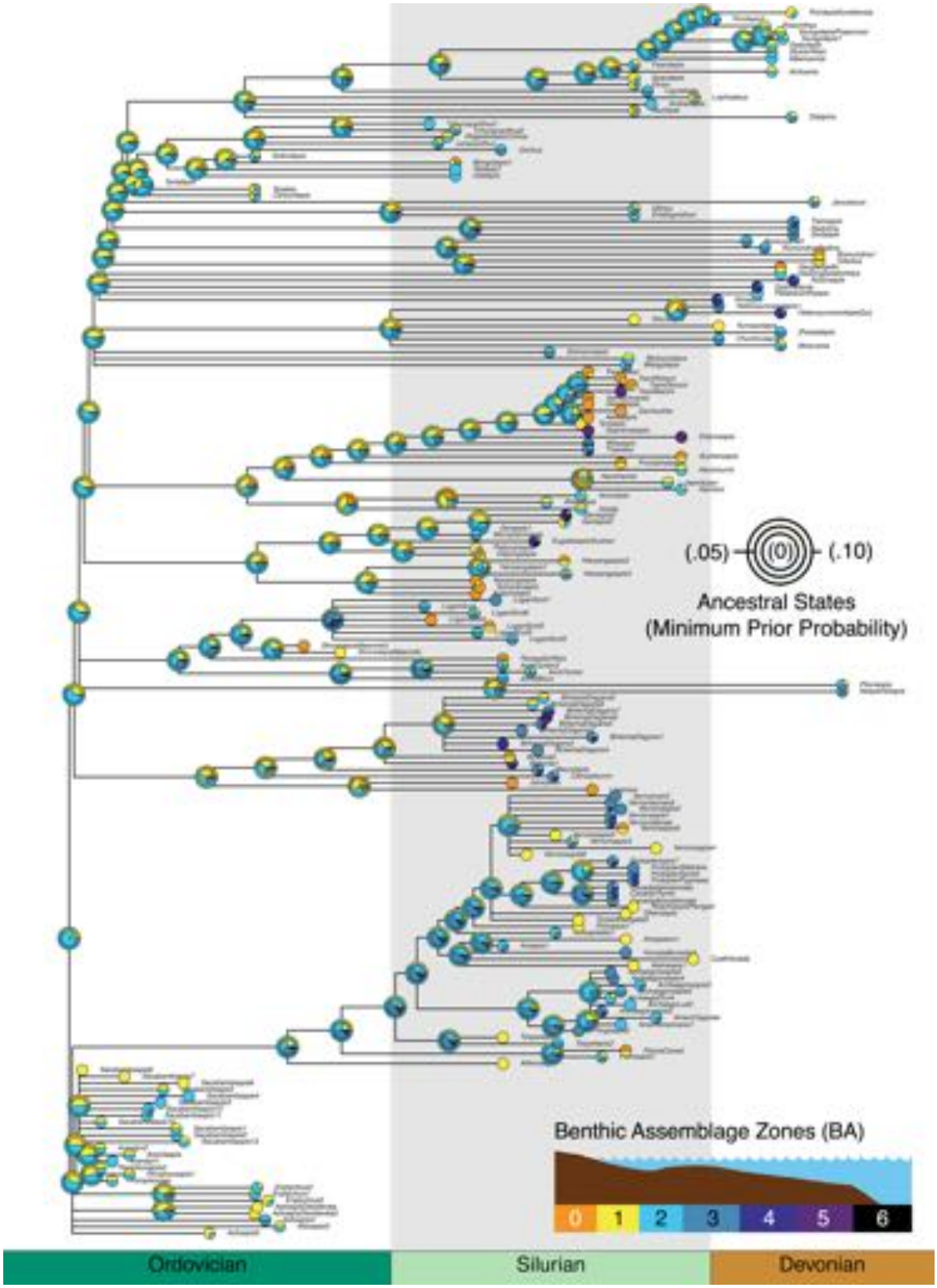
(.05)
(0)
(.10)
Ancestral States
(Minimum Prior Probability)
Benthic Assemblage Zones (BA)
0
1
2
3
4
5
6
Ordovician
Silurian
Devonian

Ancestral Habitats for Early Total-group Gnathostomes Under an Ordovician First Appearance for Jawed Fishes and Placoderm Paraphyly, Nested ancestral states represent estimations from taxon distributions with three different levels of minimum prior probability of occurrence in any bin: 0 (center, representing raw data), 0.05 (middle ring, representing moderate sampling uncertainty) and 0.10 (outer ring, representing greater sampling uncertainty). Benthic Assemblage zone key given in figure. Phylogeny based on references given in methods section. See Additional Data File S1 for tip occurrence details and Database S1 for input files, phylogenies, R code, tip ages, and all results.

Fig. S5

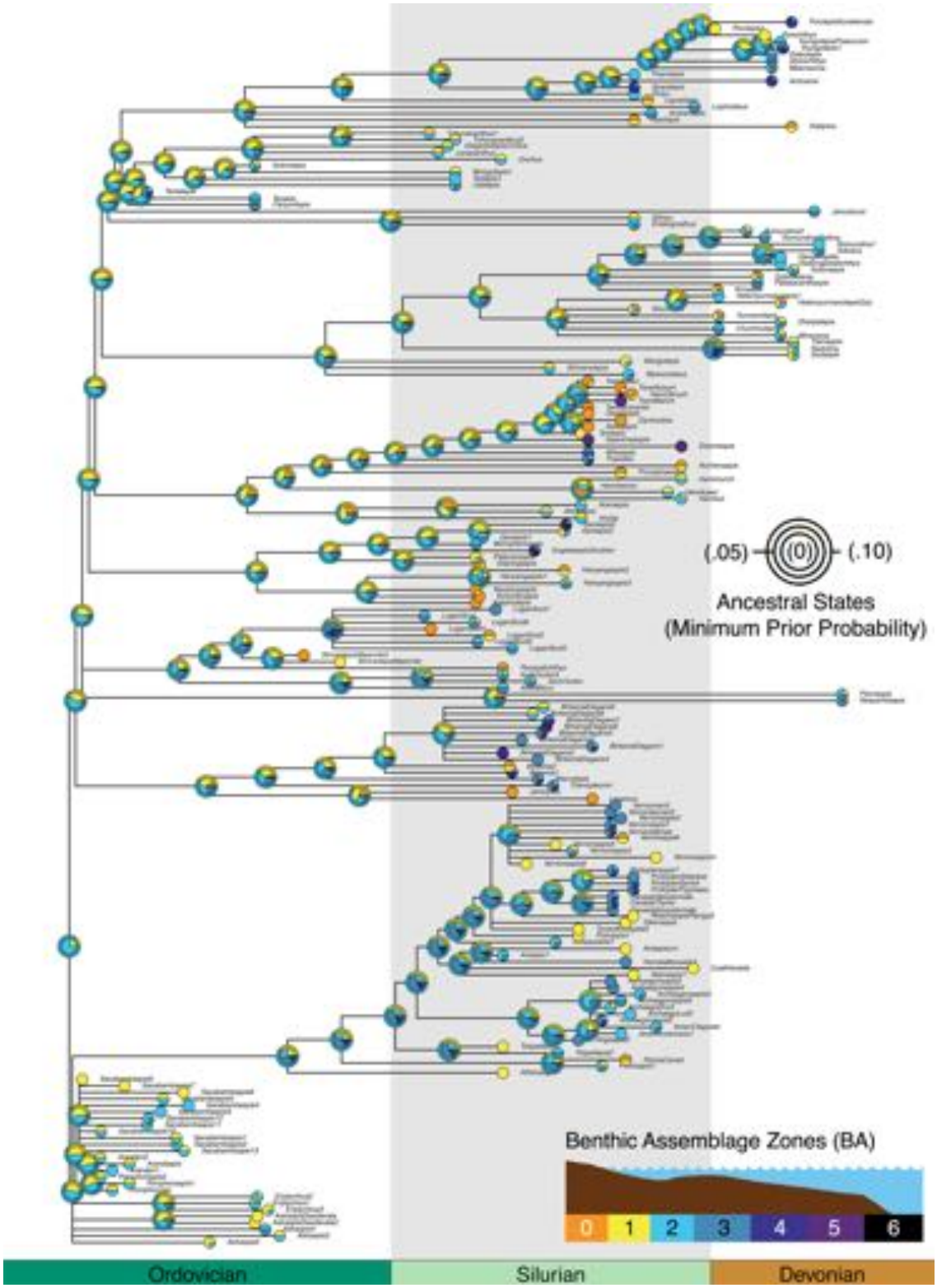

Ancestral Habitats for Early Total-group Gnathostomes Under an Ordovician First Appearance for Jawed Fishes and Placoderm Monophyly, Nested ancestral states

represent estimations from taxon distributions with three different levels of minimum prior probability of occurrence in any bin: 0 (center, representing raw data), 0.05 (middle ring, representing moderate sampling uncertainty) and 0.10 (outer ring, representing greater sampling uncertainty). Benthic Assemblage zone key given in figure. Phylogeny based on references given in methods section. See Additional Data File S1 for tip occurrence details and Database S1 for input files, phylogenies, R code, tip ages, and all results.

Fig. S6

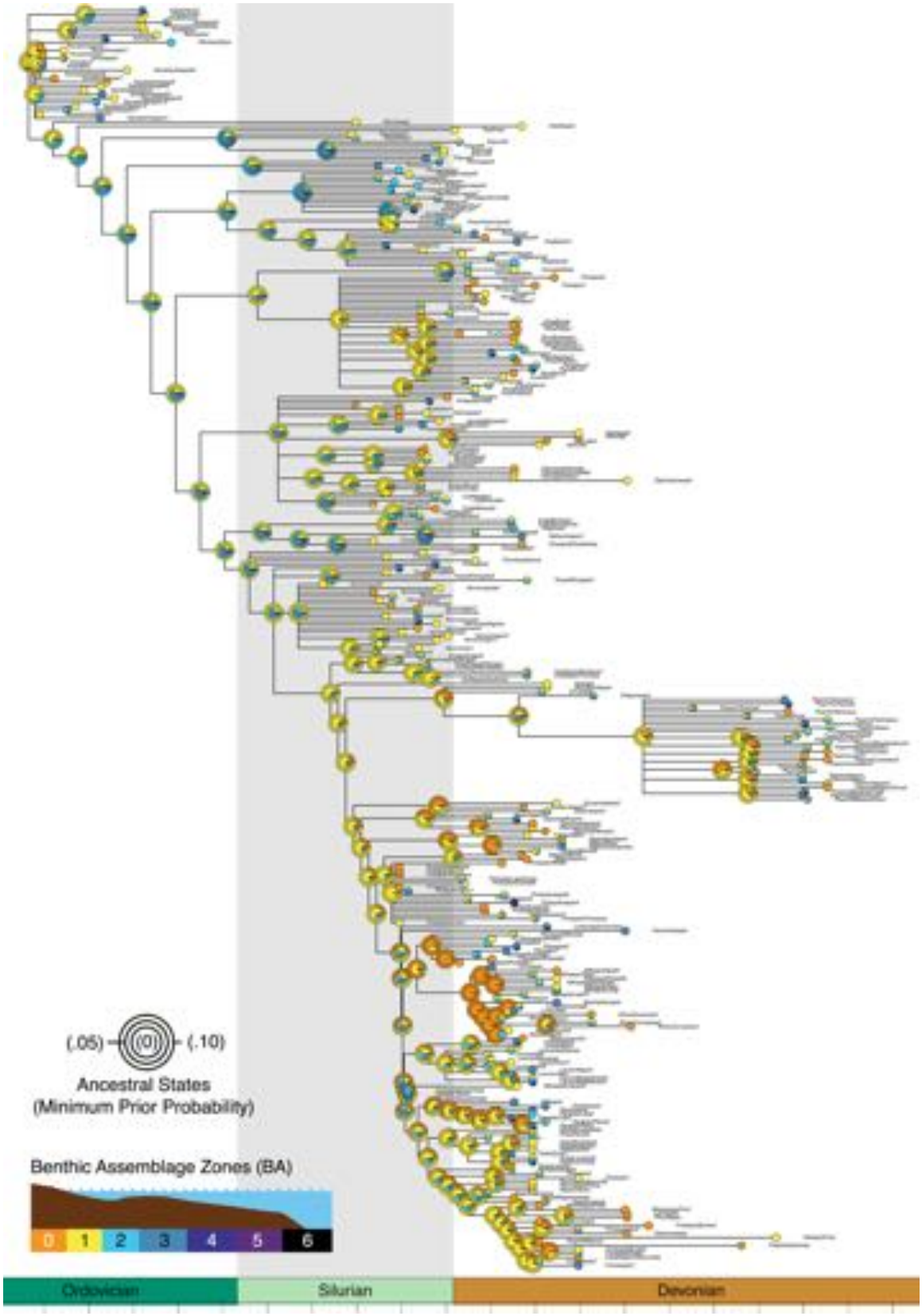
(.05)
(.10)
Ancestral States
(Minimum Prior Probability)
Benthic Assemblage Zones (BA)
0
1
2
3
4
5
6
Ordovician
Silurian
Devonian

Heterostracan Ancestral Habitats and Sampled Occurrences. Nested ancestral states represent estimations from taxon distributions with three different levels of minimum prior probability of occurrence in any bin: 0 (center, representing raw data), 0.05 (middle ring, representing moderate sampling uncertainty) and 0.10 (outer ring, representing greater sampling uncertainty). Benthic Assemblage zone key given in figure. Phylogeny based on references given in methods section. See Additional Data File S1 for tip occurrence details and Database S1 for input files, phylogenies, R code, tip ages, and all results.

Fig. S7

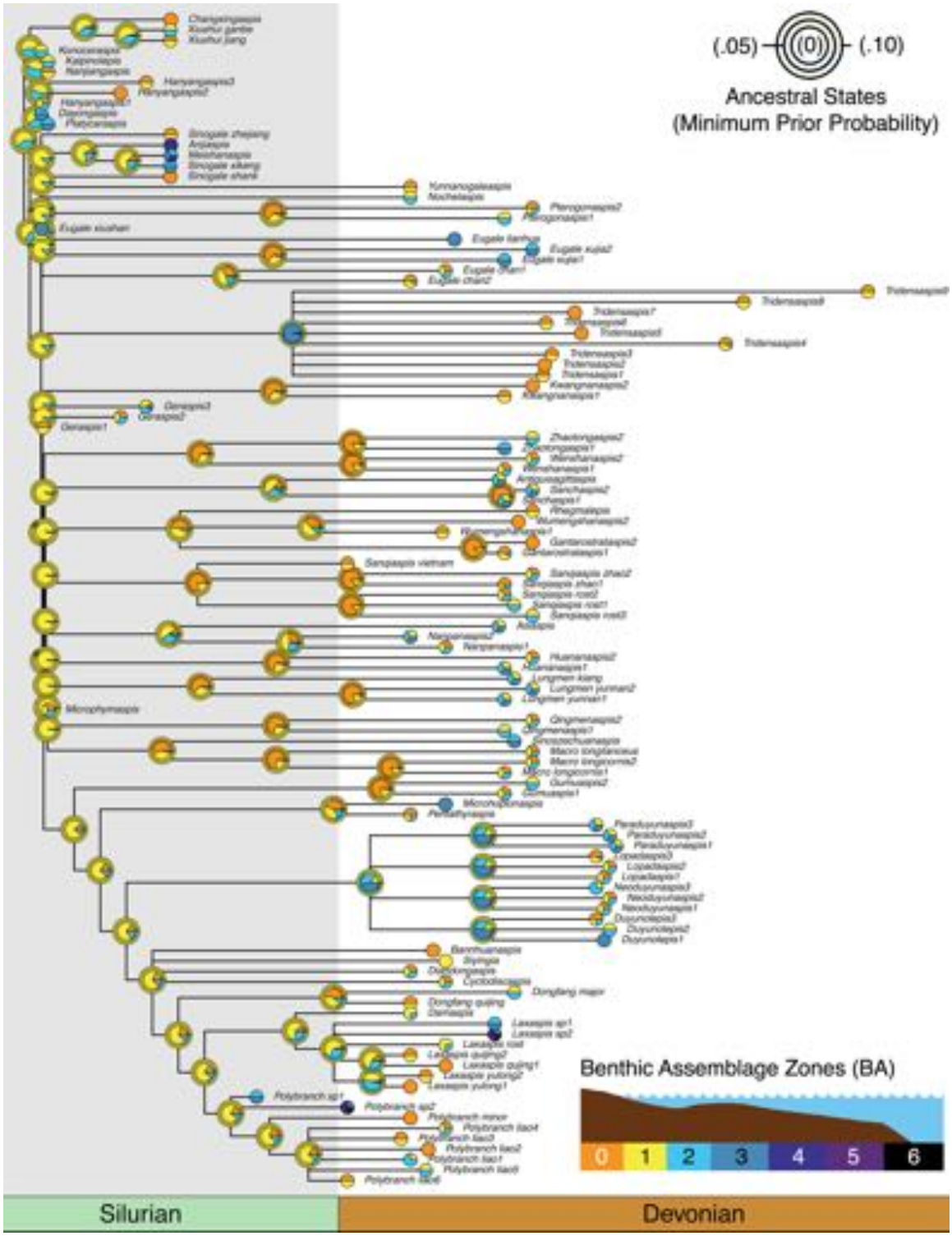

Galeaspid Ancestral Habitats and Sampled Occurrences. Nested ancestral states represent estimations from taxon distributions with three different levels of minimum prior probability of occurrence in any bin: 0 (center, representing raw data), 0.05 (middle ring, representing moderate sampling uncertainty) and 0.10 (outer ring, representing greater sampling uncertainty). Benthic Assemblage zone key given in figure. Phylogeny

based on references given in methods section. See Additional Data File S1 for tip occurrence details and Database S1 for input files, phylogenies, R code, tip ages, and all results.

.

Fig. S8

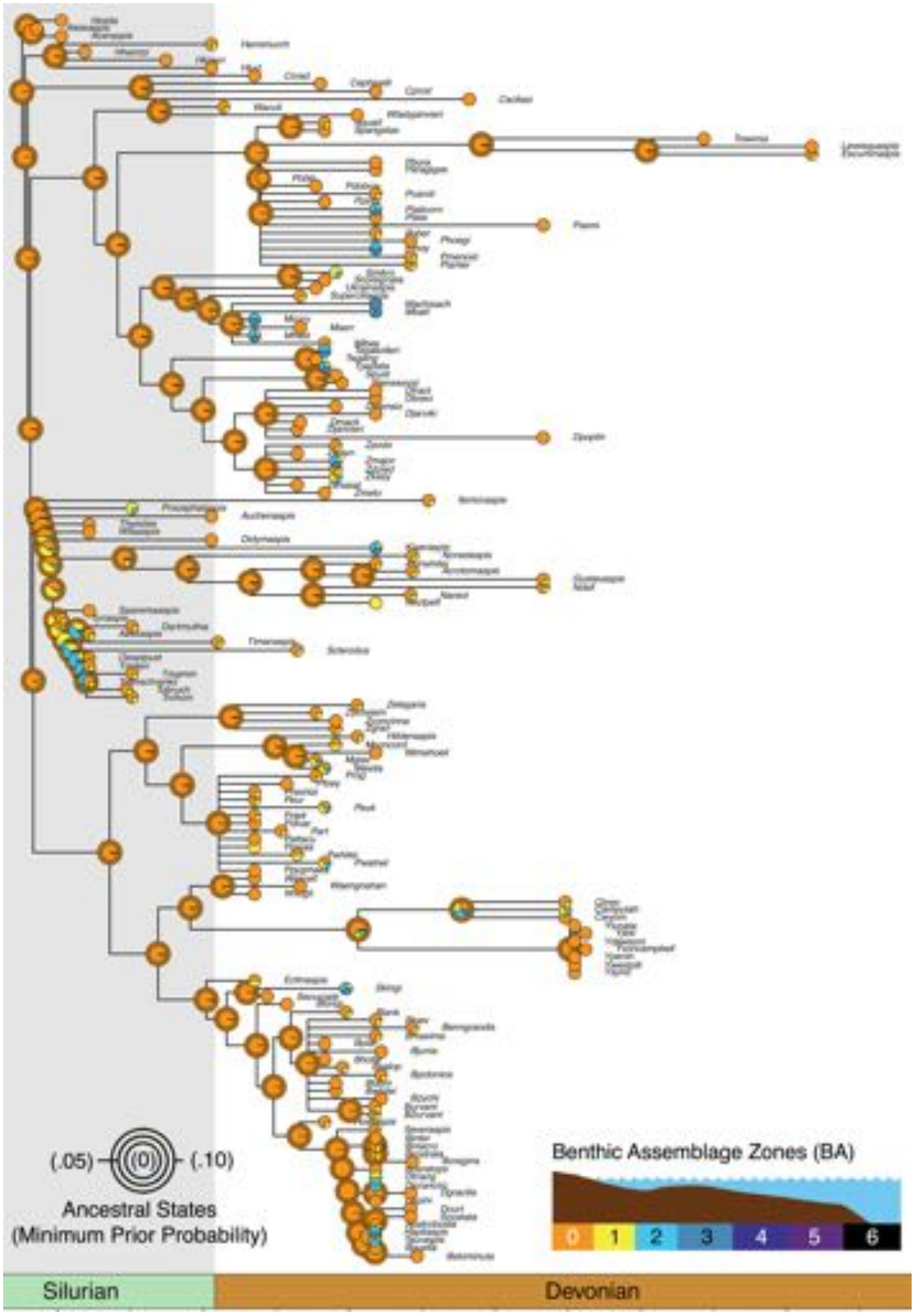
(.05)
(0)
(.10)
Ancestral States
(Minimum Prior Probability)
Benthic Assemblage Zones (BA)
0
1
2
3
4
5
6
Silurian
Devonian

Osteostracan Ancestral Habitats and Sampled Occurrences. Nested ancestral states represent estimations from taxon distributions with three different levels of minimum prior probability of occurrence in any bin: 0 (center, representing raw data), 0.05 (middle ring, representing moderate sampling uncertainty) and 0.10 (outer ring, representing greater sampling uncertainty). Benthic Assemblage zone key given in figure. Phylogeny based on references given in methods section. See Additional Data File S1 for tip occurrence details and Database S1 for input files, phylogenies, R code, tip ages, and all results.

Fig. S9

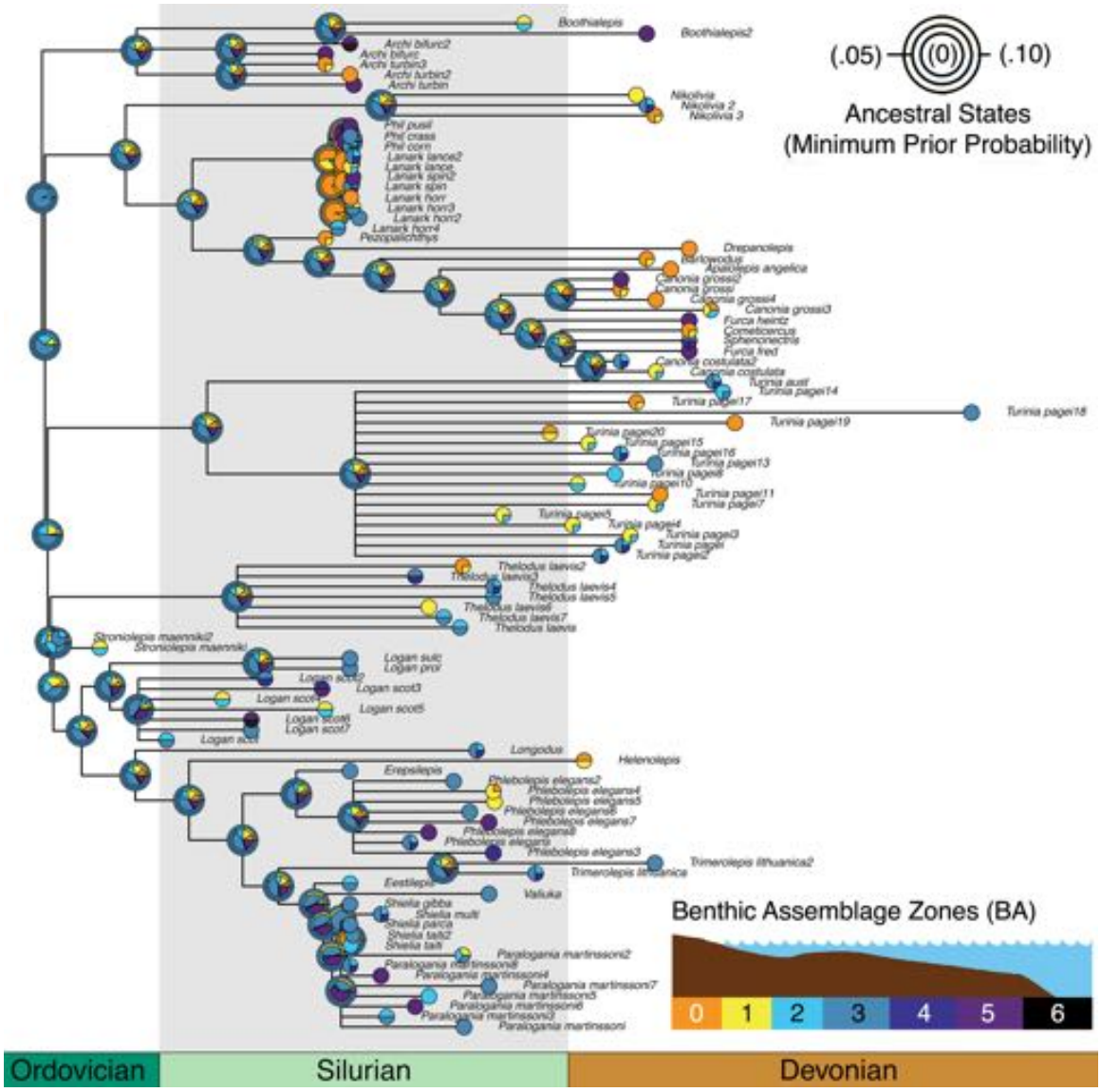

Thelodont Ancestral Habitats and Sampled Occurrences. Nested ancestral states represent estimations from taxon distributions with three different levels of minimum prior probability of occurrence in any bin: 0 (center, representing raw data), 0.05 (middle ring, representing moderate sampling uncertainty) and 0.10 (outer ring, representing greater sampling uncertainty). Benthic Assemblage zone key given in figure. Phylogeny based on references given in methods section. See Additional Data File S1 for tip occurrence details and Database S1 for input files, phylogenies, R code, tip ages, and all results.

Fig. S10

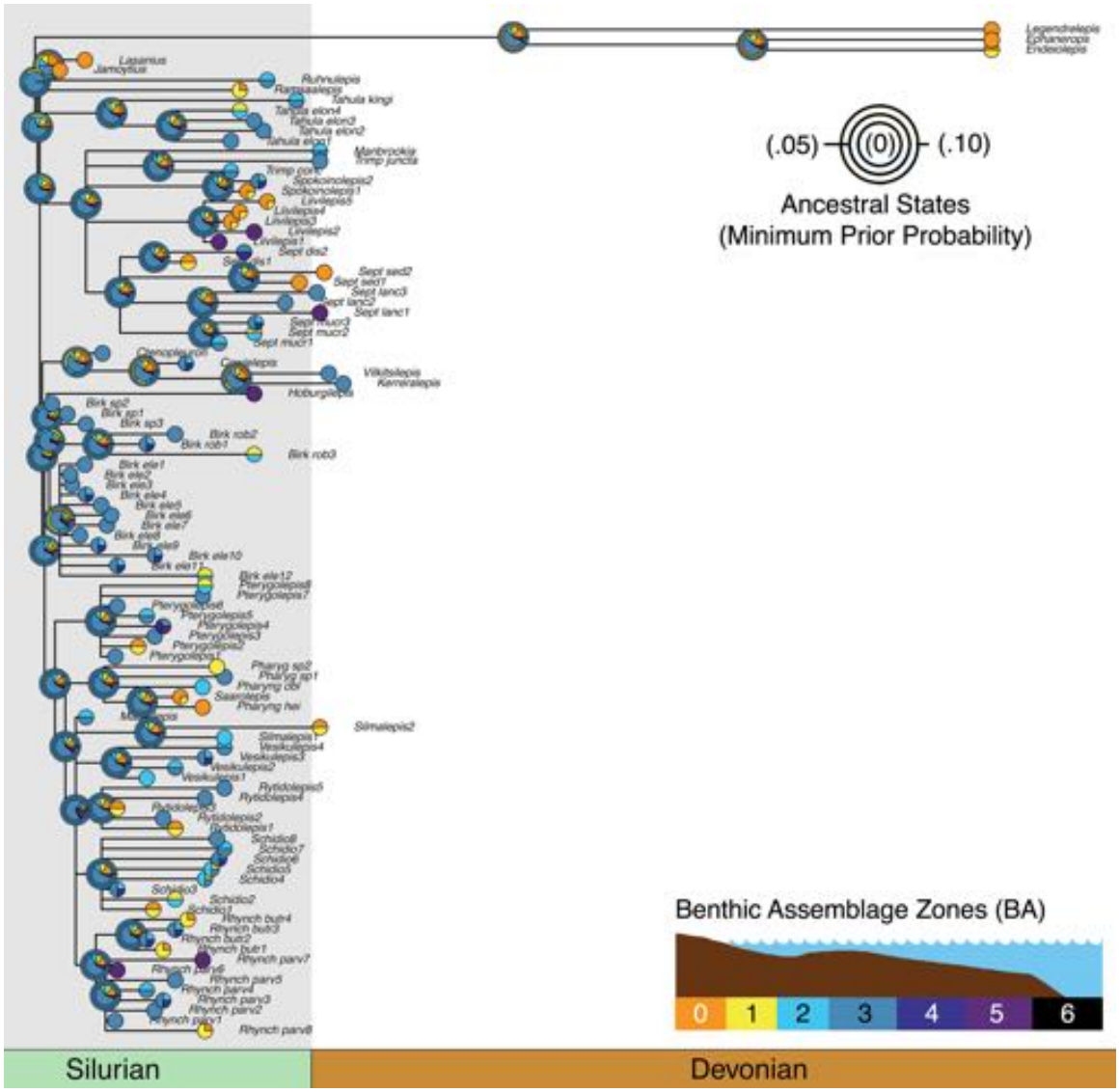

Anaspid Ancestral Habitats and Sampled Occurrences. Nested ancestral states represent estimations from taxon distributions with three different levels of minimum prior probability of occurrence in any bin: 0 (center, representing raw data), 0.05 (middle ring, representing moderate sampling uncertainty) and 0.10 (outer ring, representing greater sampling uncertainty). Benthic Assemblage zone key given in figure. Phylogenies based on references given in methods section. See Additional Data File S1 for tip occurrence details and Database S1 for input files, phylogenies, R code, tip ages, and all results.

Fig. S11

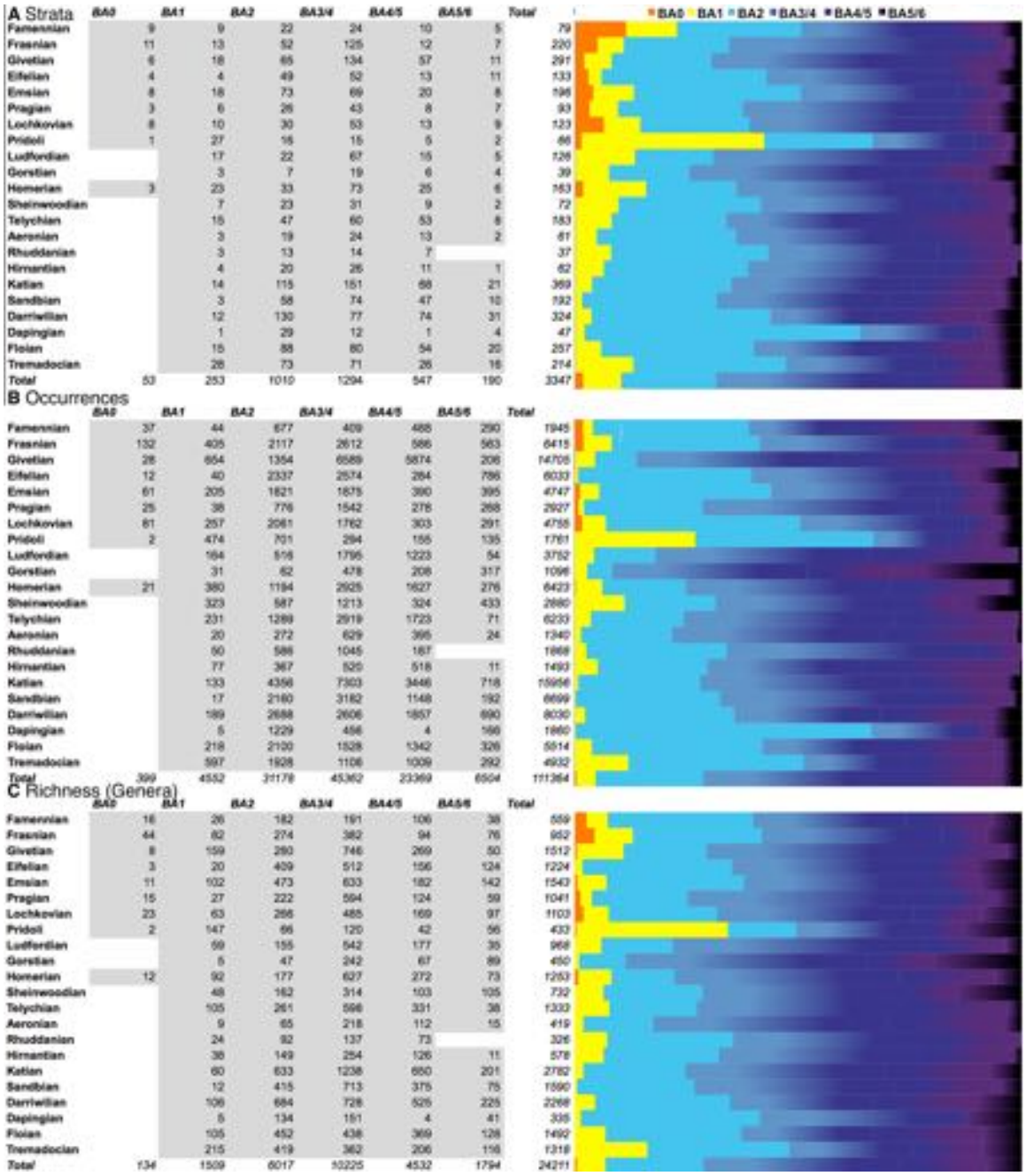

Paleobiology Database Environmental Records During the Ordovician-Devonian. Distributions by environment and stage for A) Strata, B) Occurrences, and C) Richness (Genera). Matrix shows range of occurrences by stage and counts in each Benthic Assemblage zone. Histogram shows the proportion of occurrences in each Benthic Assemblage zone by stage and overall. Paleobiology Database environmental bins may span two BA zones as described in methods but cover distinct areas of the shelf. See Additional Data File S2 for all distributions and Database S1 in Dryad for source files from the Paleobiology Database (*14*).

Fig. S12

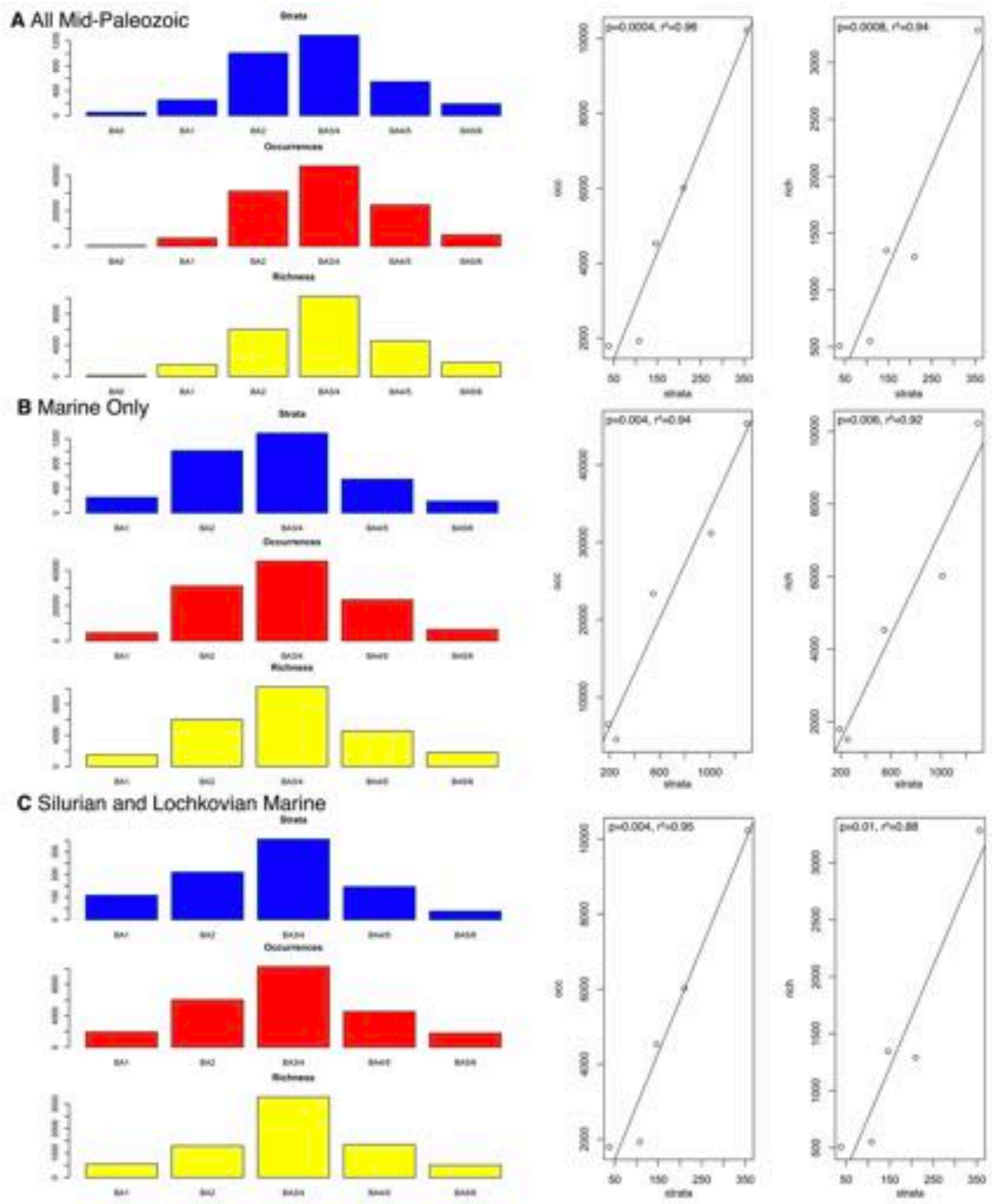

Distributions and Linear Regressions of Paleobiology Database Strata vs. Occurrences and vs. Richness A) overall, B) in marine habitats, and C) in marine Silurian and Lochkovian habitats. See Additional Data File S3 for input data and full results and Database S1 for R Code.

Fig. S13

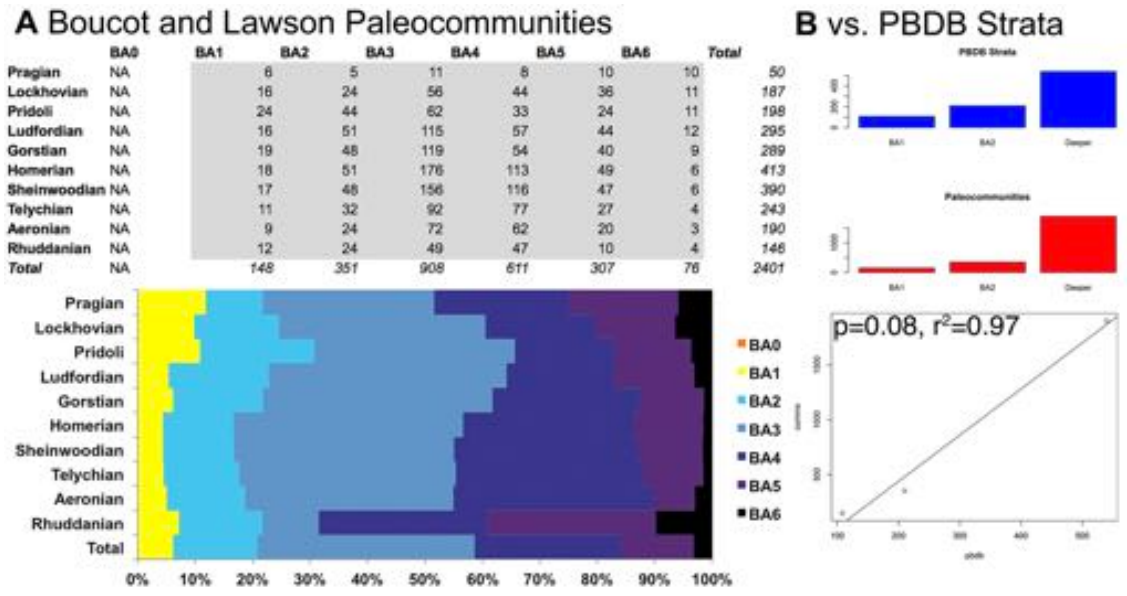

Boucot and Lawson's Silurian and Lochkovian Paleocommunities. A) Distributions of regional paleocommunities (*10*) by Benthic Assemblage zone and stage. Upper matrix shows range of occurrences by stage and counts in each BA zone. Lower histogram shows the proportion of occurrences in each Benthic Assemblage zone by stage and overall. See Additional Data File S2 for all counts and Database S1 for details on included regional paleocommunities (*10*). B) Linear regression of paleocommunities and PBDB strata (Fig. S5). Records in Benthic Assemblage zones 3-6 were pooled into the "deeper" category to account for differences in binning as explained in the methods. See Additional Data File S3 for input data and test results and Database S1 for R code.

Fig. S14

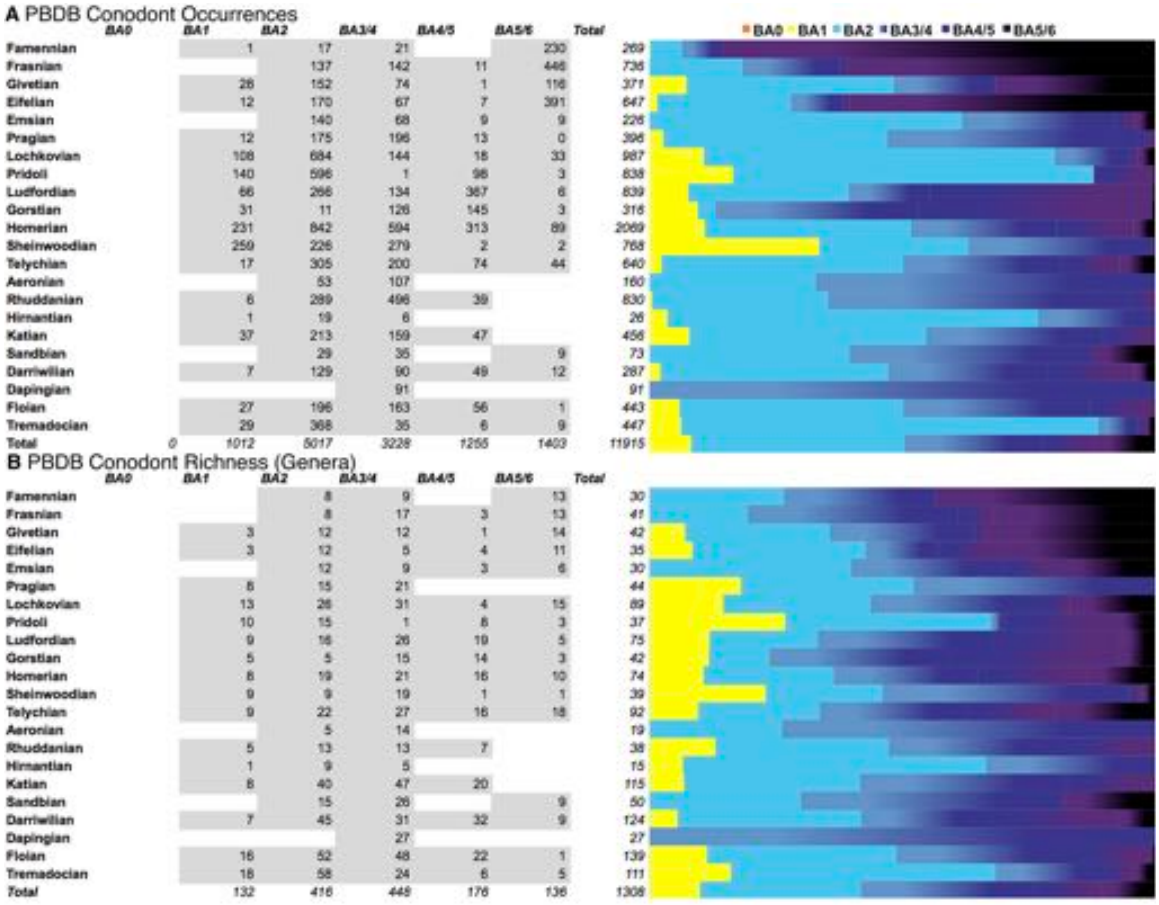

PBDB Conodont Records During the Ordovician-Devonian. Distributions of records by environment and stage for A) Strata, B) Occurrences, and C) Richness (Genera). Matrix shows range of occurrences by stage and counts in each BA zone. Histogram shows the proportion of occurrences in each Benthic Assemblage zone by stage and overall. PBDB environmental bins may span two Benthic Assemblage zones as described in methods but cover distinct areas of the shelf. See Additional Data File S2 for all distributions and Database S1 for source files from the Paleobiology Database (*14*).

Fig. S15

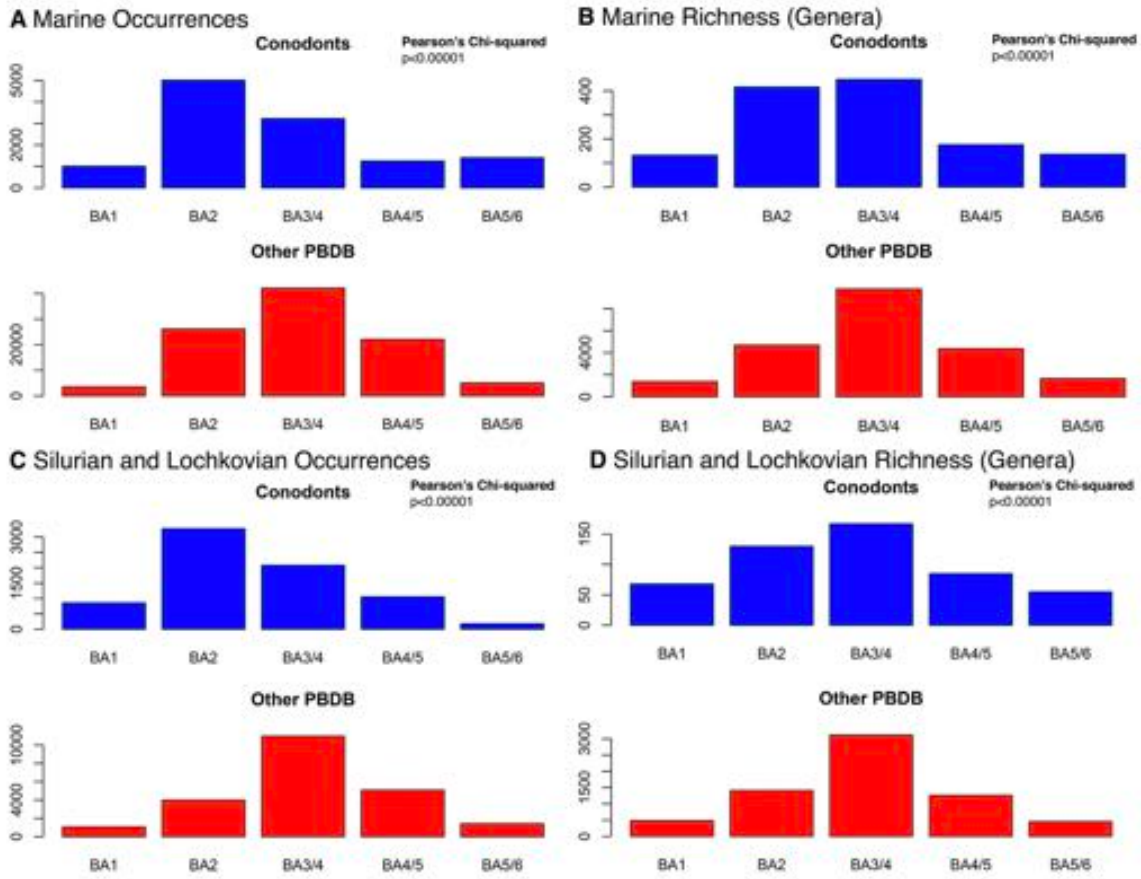

Conodont Distributions vs. Other Paleobiology Database Records. A) Marine occurrences. B) Marine richness C) Marine Silurian and Lochkovian occurrences, and D) Silurian and Lochkovian richness. Results of Pearson's Chi-squared tests shown in panel. See Additional Data File S3 for input data and full results and Database S1 for R Code.

Fig. S16

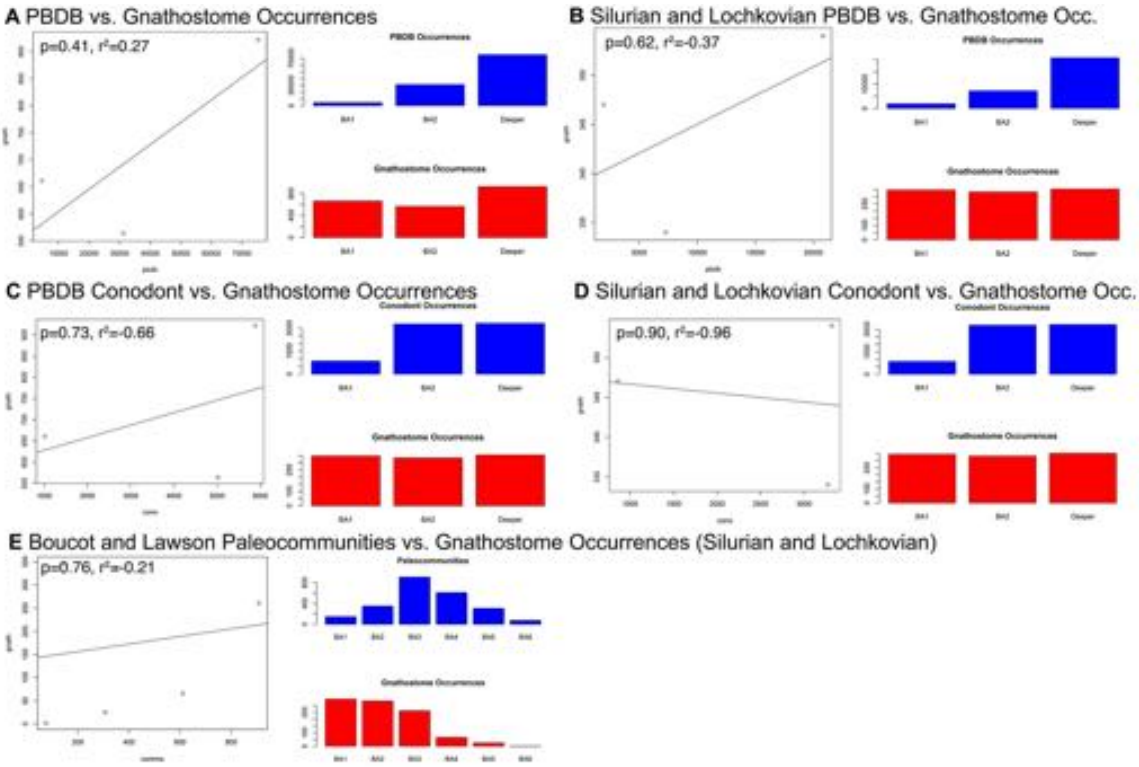

Gnathostome Distributions vs. Other Mid-Paleozoic Records. Linear regression plots shown on the left, histograms of binned records shown on the right of each panel. A) Marine Paleobiology Database occurrences vs. gnathostome occurrences. B) Silurian and Lochkovian marine Paleobiology Database occurrences vs. gnathostome occurrences. C) Marine conodont vs.gnathostome occurrences. D) Silurian and Lochkovian marine conodont vs. gnathostome occurrences. E. Boucot and Lawson's marine Silurian and Lochkovian paleocommunities vs. gnathostome occurrences. For comparisons with the PBDB, BA zones 3-6 were pooled into the “deeper” category to account for differences in binning as explained in the methods. See Additional Data File S3 for input data and full results and Database S1 for R Code.

Fig. S17

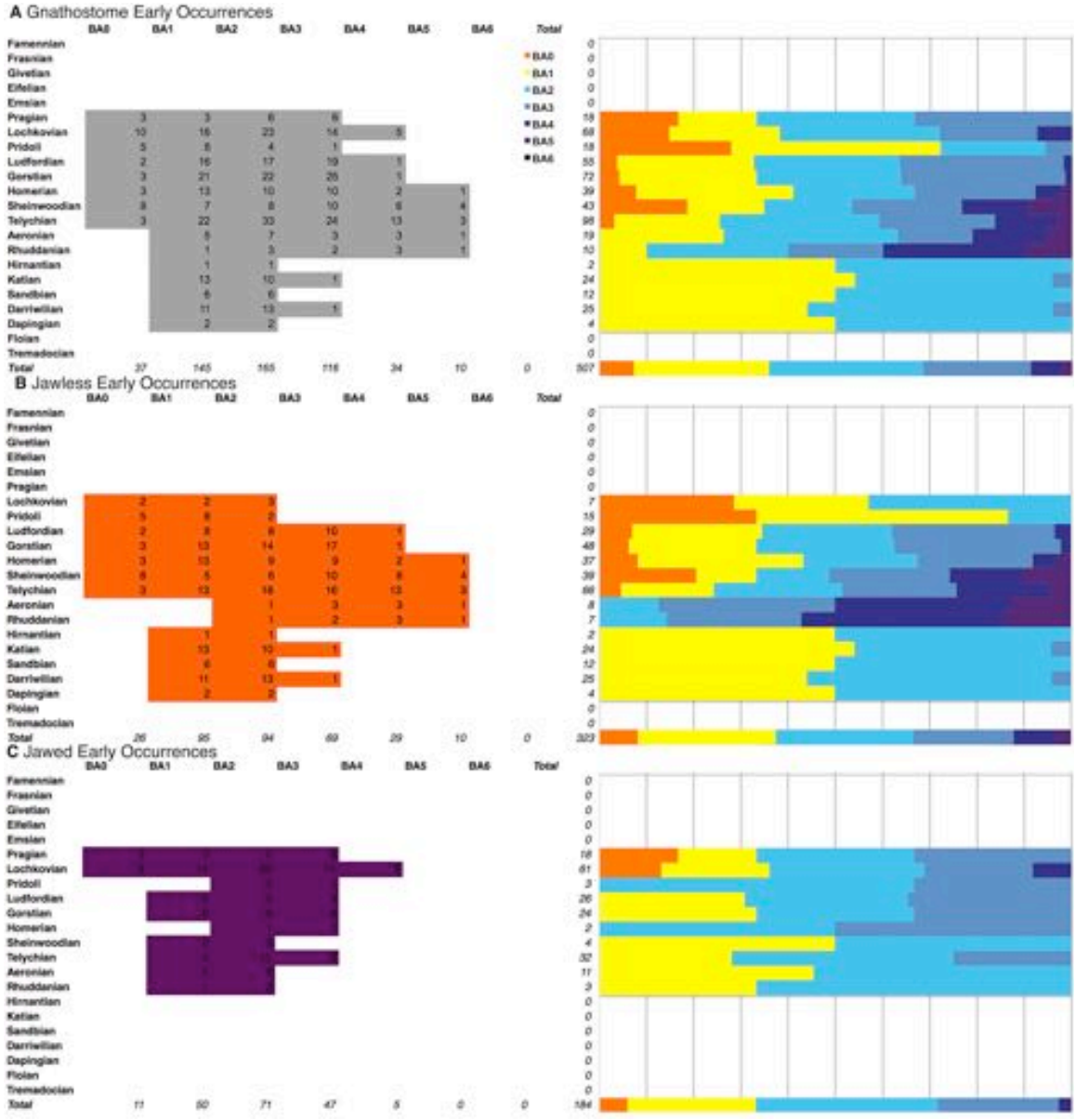

Early Occurrences for Gnathostomes Used in Ancestral State Reconstruction. A-C) Distributions of early occurrences by environment for A) Total-group Gnathostomes B) Jawless Gnathostomes and C) Jawed Gnathostomes. Early occurrences are defined as those from the five oldest localities for each major clade and those from localities with overlapping maximum ages, as detailed in the methods. Matrices on the left shows range of occurrences by stage. Histograms on the right show the proportion of occurrences in each BA zone. Detailed records available in Additional Data File S1. Exact counts in each bin available in Additional Data File S2.

Fig. S18

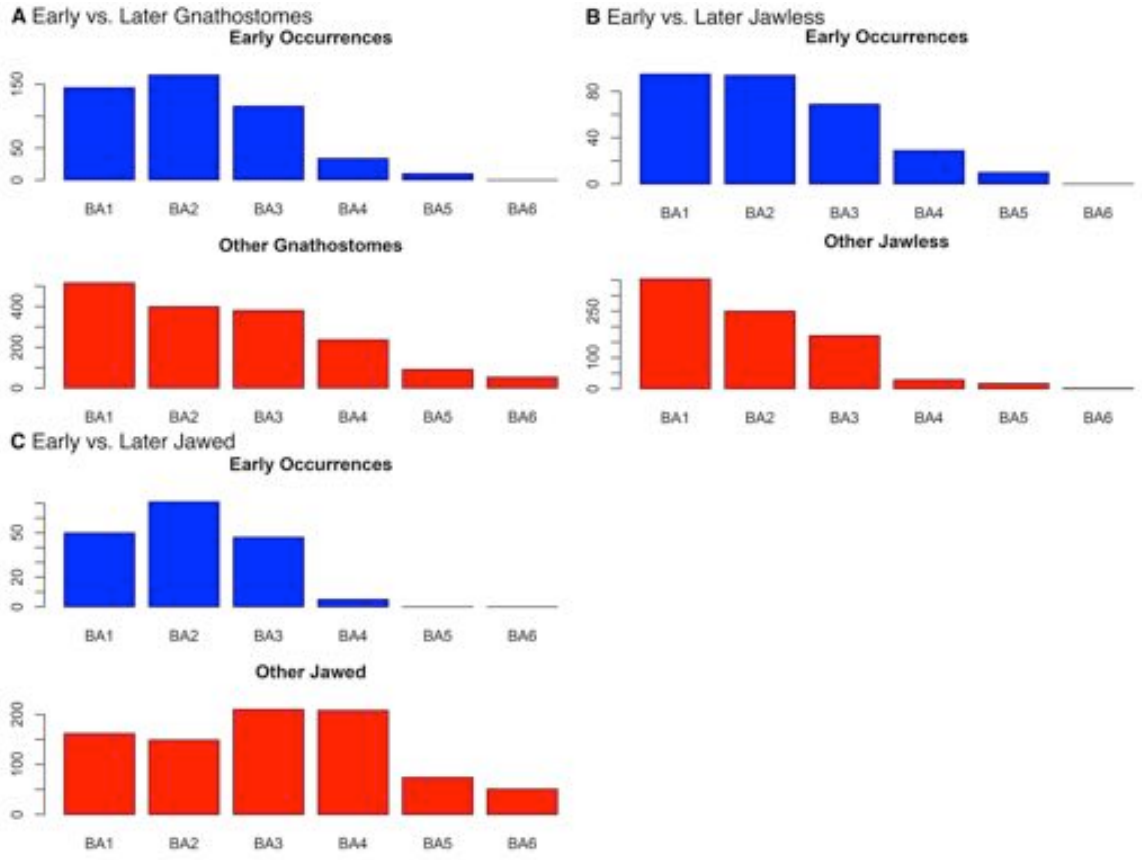

Marine Gnathostome Early Occurrences vs. Other Mid-Paleozoic Records. Linear regression plots shown on the left, histograms of binned records shown on the right of each panel. A) All Gnathostomes. B) Jawless fishes. C) Jawed fishes. Freshwater excluded to specifically test marine patterns and movement across the shelf. Results of Pearson's Chi-squared tests shown in panel. See Additional Data File S3 for input data and full results and Database S1 for R Code.

Fig. S19

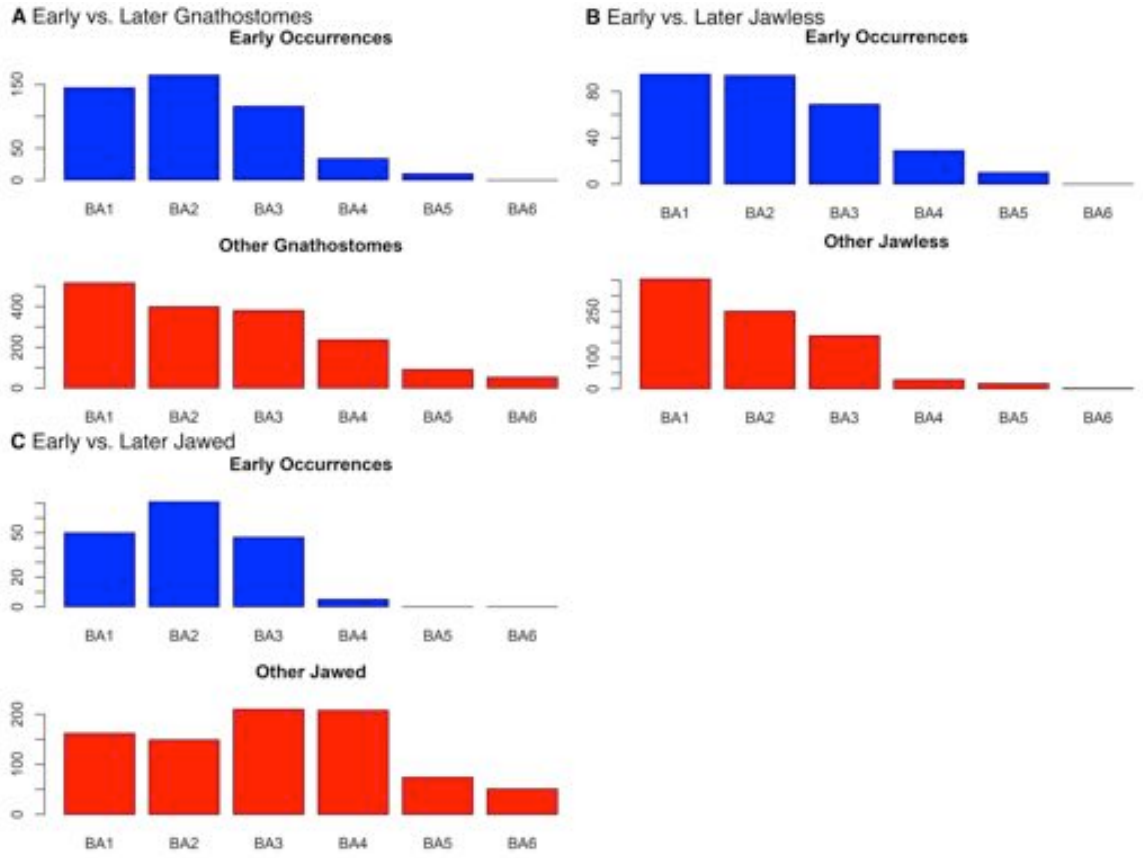

Macromeric Jawless Fish Occurrences Used in Ancestral State Reconstruction. A-C) Distributions of occurrences by environment for A) Heterostracans, B) Galeaspids, and C) Osteostracans. Early occurrences are defined as those from the five oldest localities for each major clade and those from localities with overlapping maximum ages, as detailed in the methods. Matrices on the left shows range of occurrences by stage. Histograms on the right show the proportion of occurrences in each Benthic Assemblage zone. Detailed records available in Additional Data File S1. Exact counts in each bin available in Additional Data File S2. Phylogenies and ancestral states shown in Figs. 2, S6-S8.

Fig. S20

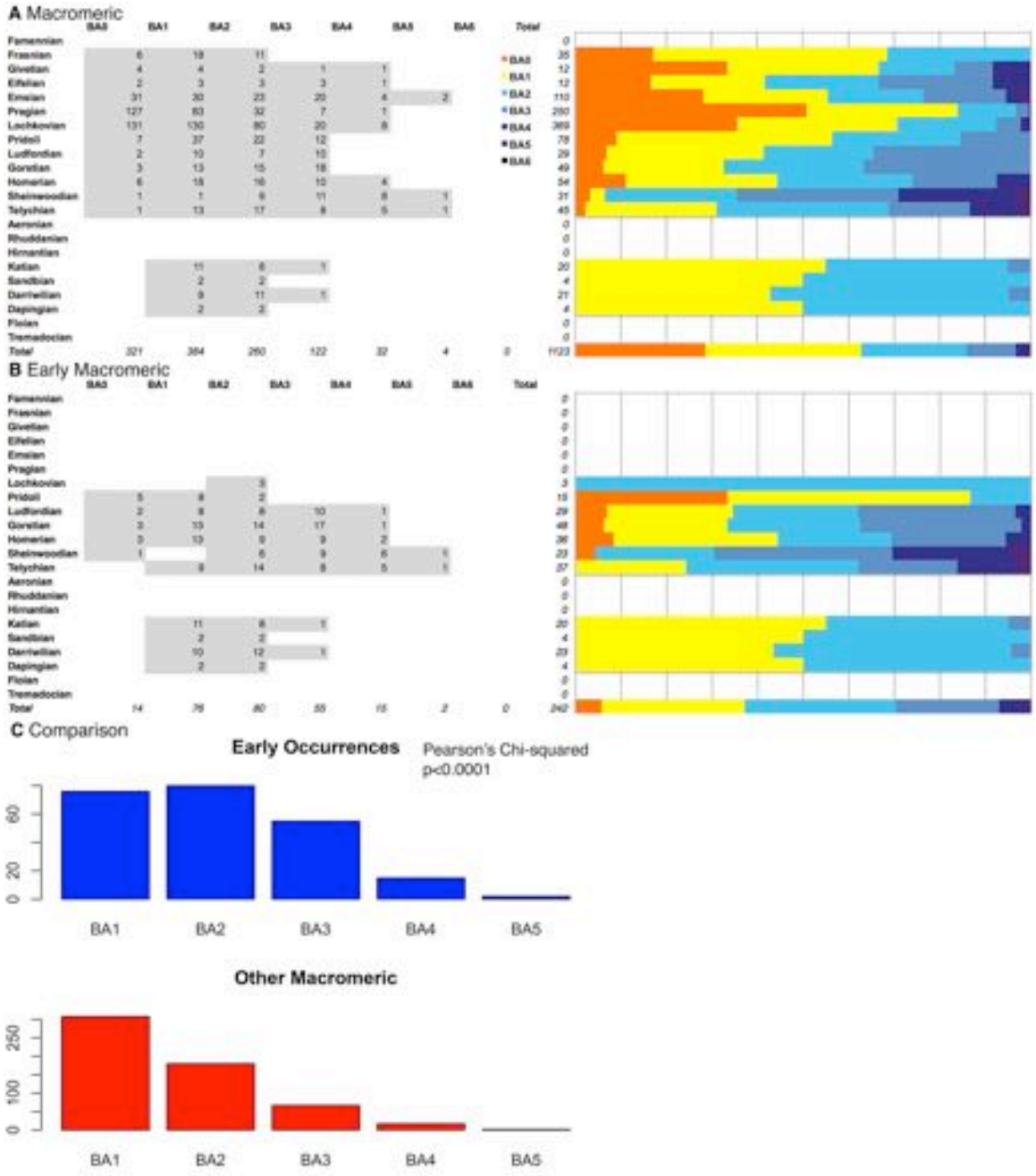

Macromeric Early Occurrences vs. Later Records. Distributions of occurrences by environment for A) All macromeric jawless fishes used in ancestral state reconstructions for clades, B) early records used in ancestral state reconstruction for all gnathostomes. C) Comparison of early and other occurrences for macromeric jawless fishes. Results of Pearson's Chi-squared tests shown in panel. Early occurrences are defined as those from the five oldest localities for each major clade and those from localities with overlapping maximum ages, as detailed in the methods. Matrices on the left shows range of occurrences by stage. Histograms on the right show the proportion of occurrences in each

Benthic Assemblage zone. Detailed records available in Additional Data File S1. Exact counts in each bin available in Additional Data File S2. Phylogenies and ancestral states shown in Figs. 1, 2, S2-S8.

Fig. S21

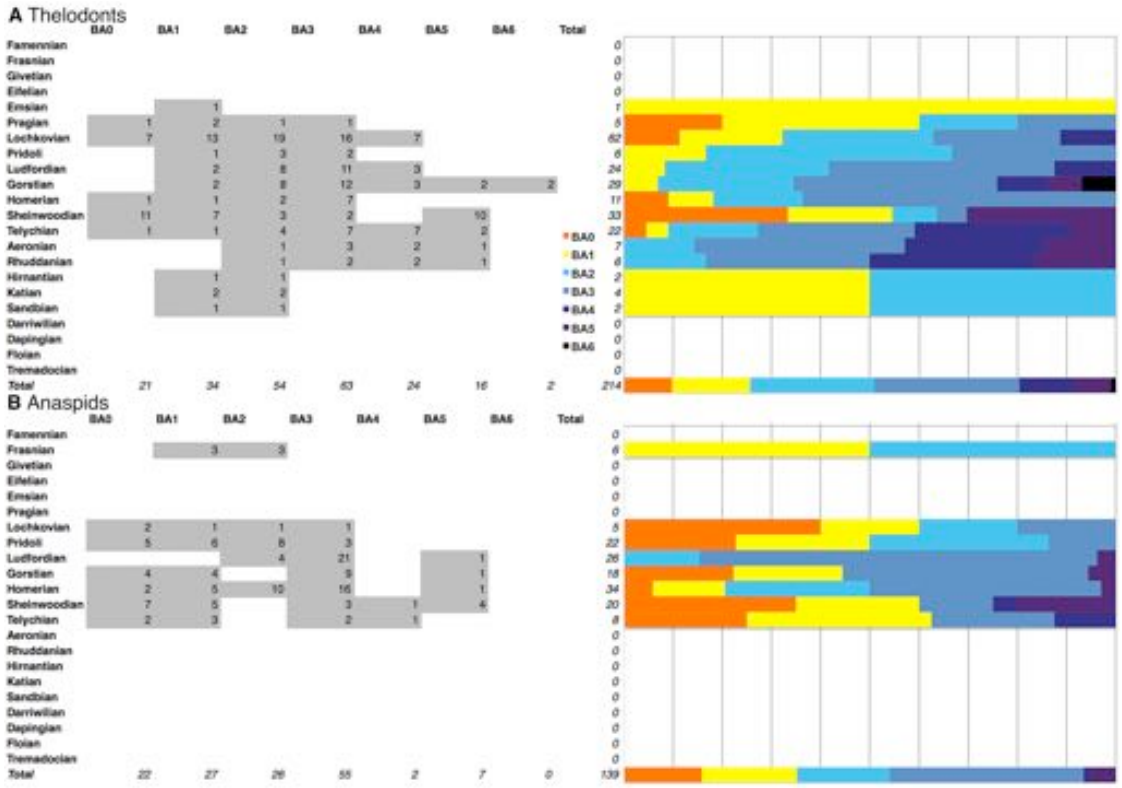

Micromeric Jawless Fish Occurrences Used in Ancestral State Reconstruction. A-B) Distributions of occurrences by environment for A) Thelodonts and B) Anaspids. Early occurrences are defined as those from the five oldest localities for each major clade and those from localities with overlapping maximum ages, as detailed in the methods. Matrices on the left shows range of occurrences by stage. Histograms on the right show the proportion of occurrences in each Benthic Assemblage zone. Detailed records available in Additional Data File S1. Exact counts in each bin available in Additional Data File S2. Phylogenies and ancestral states shown in Figs. 2, S9, S10.

Fig. S22

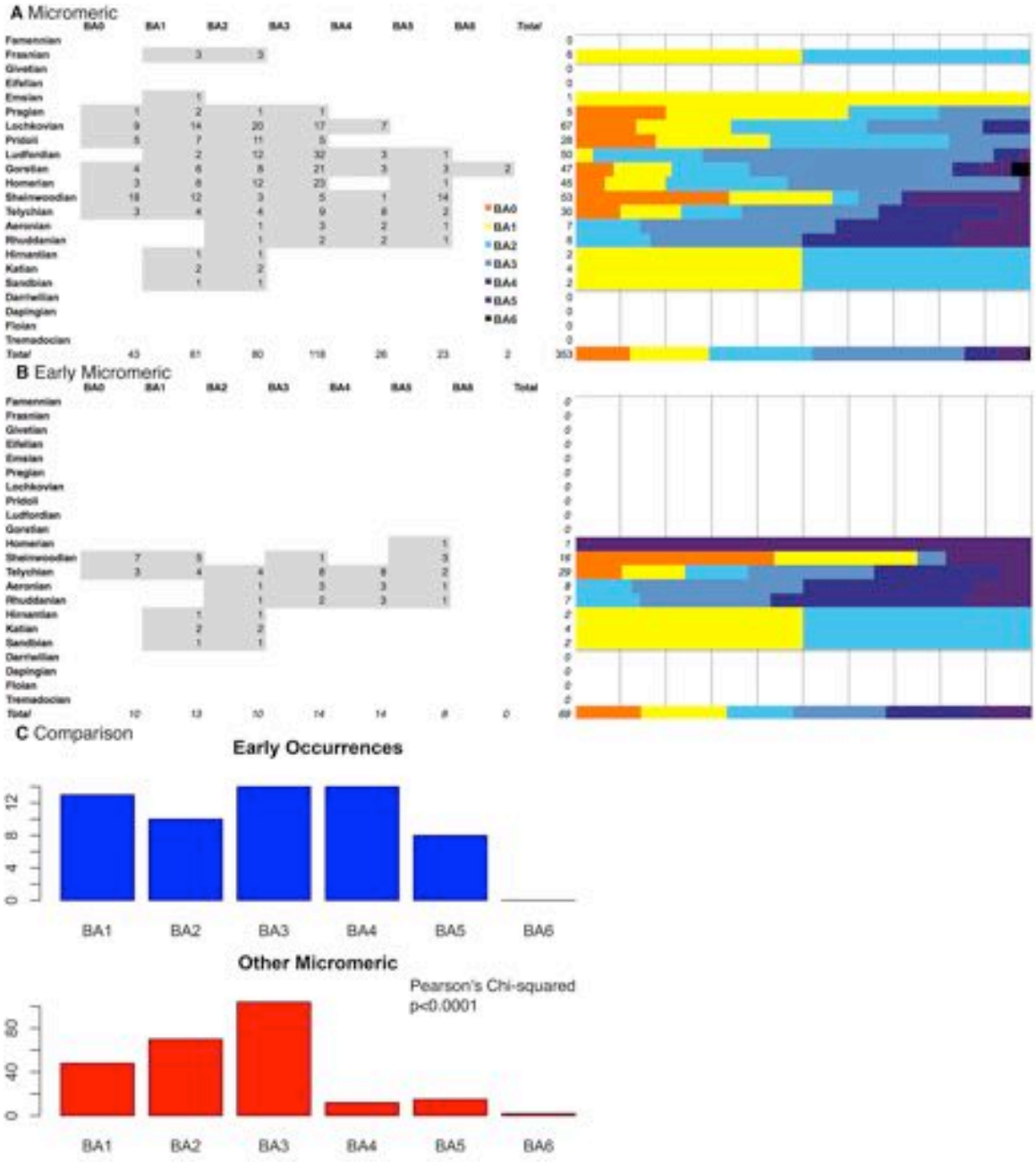

Micromeric Early Occurrences vs. Later Records. Distributions of occurrences by environment for A) All micromeric jawless fishes used in ancestral state reconstructions for clades, B) early records used in ancestral state reconstruction for all gnathostomes. C) Comparison of early and other occurrences for micromeric jawless fishes. Results of Pearson's Chi-squared tests shown in panel. Early occurrences are defined as those from the five oldest localities for each major clade and those from localities with overlapping maximum ages, as detailed in the methods. Matrices on the left shows range of occurrences by stage. Histograms on the right show the proportion of occurrences in each

Benthic Assemblage zone. Detailed records available in Additional Data File S1. Exact counts in each bin available in Additional Data File S2. Phylogenies and ancestral states shown in Figs. 1, 2, S2-S5, S9, S10.

Fig. S23

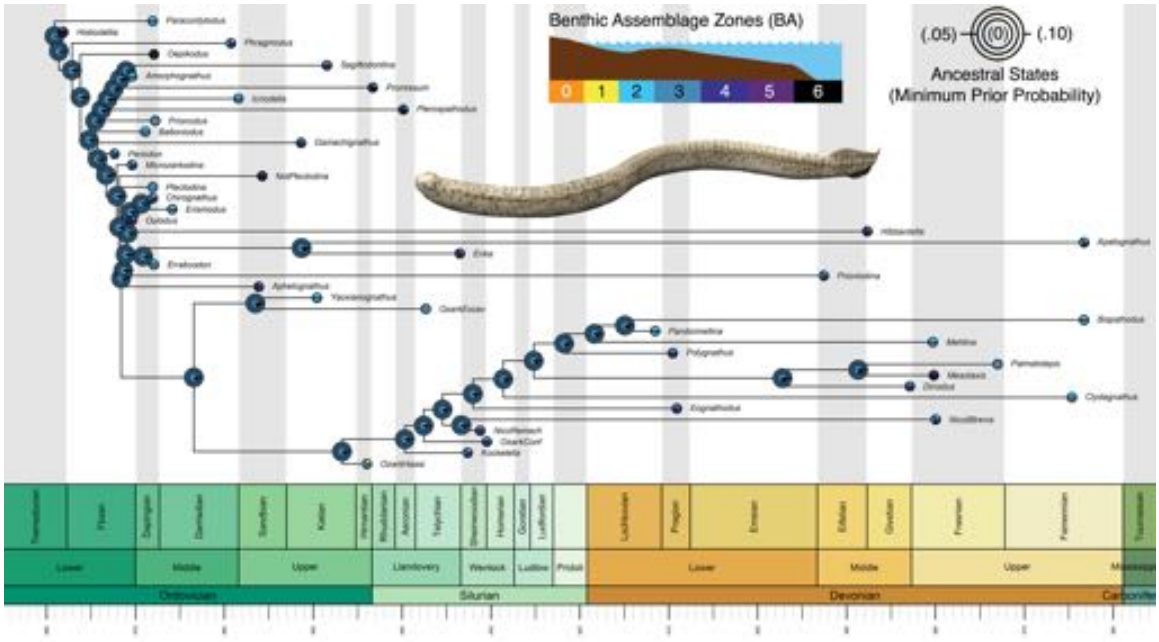

Complex Conodont Ancestral Habitats and Sampled Occurrences. Nested ancestral states represent estimations from taxon distributions with three different levels of minimum prior probability of occurrence in any bin: 0 (center, representing raw data), 0.05 (middle ring, representing moderate sampling uncertainty) and 0.10 (outer ring, representing greater sampling uncertainty). Tip values represent probabilities based on early occurrences for each genus. BA zone key given in figure. Phylogeny based on references given in methods section. See Additional Data File S1 for tip occurrence details and Database S1 for input files, phylogenies, R code, tip ages, and all results.

Table S1.

Best-Fit Model Parameters for Total-Group Gnathostomes.

AncThresh holds the threshold for exiting BA0 constant at 0, while the value for exiting BA6 is represented as Infinity, as there are no subsequent states. Values for parameters are means after excluding "burn-in." See Figs. S2-S5 and Database S1 for states.

		DIC Weights			Mean Threshold Liabilities*							Mean Parameters		
		(1 mil. gen.)			(20 mil. gen., 20% burn-in)							Log		
Topology	Min. P. Prob.	BM	OU	*L*	BA0	BA1	BA2	BA3	BA4	BA5	BA6	Likelihood	*Alpha*	Half-life
Paraphy./	0	0	1	0	0	2.09	3.98	6.24	6.81	97.48	Inf	-657.77	0.13	5.33
Silurian	0.05	0	1	0	0	5.34	10.72	30.68	62.08	122.86	Inf	-865.78	0.01	69.31
	0.1	0	1	0	0	3.96	7.82	27.02	55.59	91.78	Inf	-841.83	0.03	23.10
Monophy./	0	0	1	0	0	2.10	3.93	6.16	6.77	124.87	Inf	-659.29	0.13	5.33
Silurian	0.05	0	1	0	0	4.43	8.65	48.98	96.98	202.80	Inf	-849.39	0.02	34.66
	0.1	0	1	0	0	4.24	42.85	115.02	192.82	287.02	Inf	-647.99	2.78	0.25
Paraphy./	0	0	1	0	0	2.21	3.92	6.24	6.85	118.51	Inf	-640.46	0.13	5.33
Ordovician	0.05	0	1	0	0	5.52	11.17	35.80	80.14	184.38	Inf	-866.49	0.01	69.31
	0.1	0	1	0	0	1.99	18.29	44.33	95.09	199.36	Inf	-97.26	62.88	0.01
Monophy./	0	0	1	0	0	2.50	4.32	6.79	7.47	191.40	Inf	-662.28	0.10	6.93
Ordovician	0.05	0	1	0	0	0.46	0.62	29.02	67.83	149.82	Inf	-49.29	47.68	0.01
	0.1	0	1	0	0	0.80	28.88	61.13	137.28	187.56	Inf	-77.16	70.69	0.01

Table S2.

Best-Fit Model Parameters for Macromeric Jawless Gnathostomes.

AncThresh holds the threshold for exiting BA0 constant at 0, while the value for exiting BA6 is represented as Infinity, as there are no subsequent states. Values for parameters are means after excluding "burn-in." See Fig. S6-S8 and Database S1 for states.

		DIC Weights			Mean Threshold Liabilities*							Mean Parameters		
	Min.	(1 mil. gen.)			(20 mil. gen., 20% burn-in)							Log		
Clade	P. Prob.	BM	OU	*Lambda*	BA0	BA1	BA2	BA3	BA4	BA5	BA6	Likelihood	*Alpha*	Half-life (My)
Heterostracans	0	0	1	0	0	2.92	3.86	7.74	38.20	200.13	Inf	-979.86	0.12	5.78
	0.05	0	1	0	0	9.40	13.07	42.58	75.53	186	Inf	-1139.70	0.003	231.05
	0.1	0	1	0	0	15.28	30.73	81.35	135.39	223.4	Inf	-1476.72	0.01	69.31
Galeaspids	0	0.07	0.93	<0.01	0	3.31	5.91	15.53	83.03	200.55	Inf	-446.63	0.005	138.63
	0.05	<<0.01	~1	<<0.01	0	5.31	14.27	49.53	94.78	191.63	Inf	-497.53	0.005	138.63
	0.1	<<0.01	~1	<<0.01	0	16.48	35.83	62.56	102.83	157.89	Inf	-496.41	0.14	4.95
Osteostracans	0	<<0.01	~1	<<0.01	0	1.13	2.90	26.27	51.66	94.34	Inf	-433.09	0.08	8.66
	0.05	<<0.01	~1	<<0.01	0	19.23	41.12	66.36	114.27	162.78	Inf	288.78	374.53	0.00
	0.1	<<0.01	~1	0	0	15.89	33.88	56.14	99.07	208.52	Inf	275.56	469.92	0.00

Table S3.

Best-Fit Model Parameters for Micromeric Gnathostomes and Complex Conodonts. *AncThresh* holds the threshold for exiting BA0 constant at 0, while the value for exiting BA6 is represented as Infinity, as there are no subsequent states. Values for parameters are means after excluding "burn-in." See Figs. S9, S11 and Database S1 for ancestral states.

		DIC Weights			Mean Threshold Liabilities*							Mean Parameters		
	Min.	(1 mil. gen.)			(20 mil. gen., 20% burn-in)							Log		
Clade	P. Prob.	BM	OU	*Lambda*	BA0	BA1	BA2	BA3	BA4	BA5	BA6	Likelihood	*Alpha*	Half-life (My)
Anaspids	0	<<0.01	~1	<<0.01	0	0.19	0.34	1.35	1.40	103.24	Inf	-142.24	1.95	0.36
	0.05	0.76	0.24	<<0.01	0	0.81	1.29	47.95	94.61	183.75	Inf	-380.70	NA	NA
	0.1	<<0.01	~1	<<0.01	0	0.85	1.71	30.29	74.96	160.18	Inf	15.64	149.87	0.00
Thelodonts	0	<<0.01	~1	<<0.01	0	0.61	0.93	2.05	2.15	110.77	Inf	-220.20	0.59	1.17
	0.05	<<0.01	~1	<<0.01	0	1.66	2.36	36.19	85.20	155.15	Inf	-388.72	0.14	4.95
	0.1	<<0.01	~1	<<0.01	0	1.13	2.26	46.27	99.87	194.34	Inf	26.93	194.30	0.00
		DIC Weights			Mean Threshold Liabilities							Mean Parameters		
	Min.	(1 mil. gen.)			(50 mil. gen., 20% burn-in)							Log		
Clade	P. Prob.	BM	OU	*Lambda*	BA0	BA1	BA2	BA3	BA4	BA5	BA6	Likelihood	*Alpha*	Half-life (My)
Conodonts	0	<<0.01	~1	<<0.01	0	4.73	9.94	21.23	21.77	21.90	Inf	-134.23	4.29	0.16
	0.05	<<0.01	~1	<<0.01	0	1.45	2.96	34.99	81.20	185.93	Inf	112.36	749.15	0.00
	0.1	<<0.01	~1	<<0.01	0	0.75	1.50	26.86	72.21	157.52	Inf	76.90	363.90	0.00

Additional Data Table S1 (separate file)

Mid-Paleozoic Gnathostome Occurrences. Detailed occurrence records and references for mid-Paleozoic occurrences used in phylogenetic comparative methods and statistical analyses.

Additional Data Table S2 (separate file)

Mid-Paleozoic Habitat Distributions. Records from the Paleobiology Database (14), Boucot and Lawson (10) and mid-Paleozoic gnathostomes binned by stage and BA zone. See Additional Data Table S1 and Database S1 for source data and details.

Additional Data Table S3 (separate file)

Statistical Comparisons. Input data and results for statistical comparisons of habitat distributions. See Additional Data Table S2 for full data and Database S1 for R code.

Database S1 (separate file on Dryad)

All Other Data, Input Files, Code and Results. All Paleobiology Database and paleocommunity datasets, input files, R code, and results for analyses. (doi:10.5061/dryad.g08m87q)